PHYSICAL REVIEW C VOLUME 8, NUMBER 5 NOVEMBER 1973

Study of Even-Odd Nuclei with N or $Z = 11$ and 13

M. Lambert and P. Midy*
Institut de Physique Nucléaire, Université Claude Bernard de Lyon-I 43, Bd. du 11 novembre 1918, 69621 Villeurbanne, France

P. Desgrolard
Institut d'Etudes Nucléaires, Alger, Algérie

(Received 24 October 1972; revised manuscript received 7 May 1973)

The 10 even-odd nuclei with an odd number of nucleons, $\xi = 11$: ^{19}O, ^{21}Ne, ^{21}Na, ^{23}Na, ^{23}Mg; and $\xi = 13$: ^{23}Ne, ^{25}Mg, ^{25}Al, ^{27}Al, ^{27}Si have been studied in the framework of the Bohr-Mottelson and Nilsson models. Two different methods of calculation have been used for the energies and wave functions of positive- and negative-parity states. The ground-state static moments and $M1$-$E2$ transition rates have been computed. A minimum number of phenomenological parameters have been used. It has been confirmed that these nuclei (except ^{19}O) show an equilibrium prolate deformation and can be well accounted for by the model, especially as concerns the positive-parity particle states. Difficulties arise for most of the hole states and negative-parity particle states. Parameters are found to be in the same range for all nuclei. General conclusions on the validity of the model have been discussed in the lower part of the $2s$-$1d$ shell.

I. INTRODUCTION

It seems at present well established that most of the nuclei in the lower $2s$-$1d$ shell show an equilibrium deformation and that the properties of their first excited levels can successfully be understood in the description of the Bohr-Mottelson[1] and Nilsson[2] models. These models have been the most extensively used until now and are still of interest though they are now two decades old. The reasons for this are the following:

(i) Though they are very simple and with an elementary theoretical structure, they very often yield predictions in good agreement with the experimental data.

(ii) The number of fitting parameters used in these phenomenological models can be reduced to three or four for a given nucleus. This is less than in other "microscopic," and therefore more fundamental, models.

(iii) The results obtained within the framework of these phenomenological models can be used as a starting point in a calculation aiming at a better approximation. For example, the Nilsson eigenfunctions of the occupied states can be used as a starting point in an iterative Hartree-Fock-type calculation.

However, most of the previous studies (except some of them[3,4] which are now rather old) concern only one or two mirror pair nuclei or very often some particular properties of a given nucleus (e.g., one rotational band of a given nucleus). Thus, even if the number of fitting parameters is not increased as is often done (energies of the rotational band heads adjusted to the experimental values, for example), it is easier to obtain a better agreement with the experiment. But this agreement is far less significant because the values given to the parameters must change with the nucleus and, in addition, with the properties of a given nucleus to be reproduced.

We thought it of interest to present a more general and stricter application of these phenomenological models, because the abundance of currently available experimental data allows a more complete comparison with the theoretical predictions. The present investigation deals with the 10 even-odd nuclei with an odd number of nucleons (N or Z) $\xi = 11$, namely: ^{19}O, ^{21}Ne, ^{21}Na, ^{23}Na, ^{23}Mg; and $\xi = 13$: ^{23}Ne, ^{25}Mg, ^{25}Al, ^{27}Al, ^{27}Si. For these 10 nuclei, we attempt an interpretation of the experimental results concerning (i) the positive- and negative-parity energy levels and their spectroscopic factors of stripping reactions [(d, p), (^{3}He, d), ...], (ii) the static moments of the ground state, and (iii) the electromagnetic transitions between particle states with positive parity (branching ratios, $E2/M1$ mixing ratios and mean lifetimes).

For each nucleus, we tentatively look for a minimum number of parameters with reasonable physical values reproducing the whole of the above properties.

To realize this program, two completely independent calculations have been made according to two possible interpretations in the practical utilization of the Bohr-Mottelson and Nilsson models. The mixing of the rotational bands due to the Coriolis coupling term is introduced in both methods of calculation. In the first calculation the deformation is one of the parameters, but in the second calculation its value is fixed by the requirements of a stable configuration. The formalism

and a summary of the detailed calculations in both methods are given in Sec. II. The results for the five $\xi = 11$ nuclei are successively given and discussed in Sec. III and those for the five $\xi = 13$ nuclei in Sec. IV. Finally, general concluding remarks are deduced in Sec. V.

II. NUCLEAR MODEL: DETAILS OF THE CALCULATIONS

A. First Description of the Energy Levels

In this first application of the Bohr-Mottelson and Nilsson models (denoted hereafter as TH.I), the outer nucleon is strongly bound in the deformed well created by the even-even core which is assumed to be axially symmetric, rigid, and without any surface vibration. The Hamiltonian includes a term (H_p) representing the motion of the single nucleon and a term (H_R) describing the rotation of the core:

$$H = H_p + H_R . \tag{1}$$

The unpaired nucleon is supposed to be dragged along with the Nilsson potential[2] described in the rotating core set of coordinates (x, y, z) by

$$H_p = -\frac{\hbar^2}{2m}\nabla^2 + \tfrac{1}{2}m(\omega_\perp{}^2x^2 + \omega_\perp{}^2y^2 + \omega_\parallel{}^2z^2) + C\vec{l}\cdot\vec{s} + Dl^2 , \tag{2}$$

where m, $\vec{s}$ ($s = \frac{1}{2}$), and $\vec{l}$ stand respectively for the mass, the spin of the nucleon, and the relative orbital angular momentum; C and D are constants. If this Hamiltonian is written in the δ representation of Nilsson[2] the pulsations are then

$$\omega_\perp = \omega_0(1+\tfrac{2}{3}\delta)^{1/2}, \quad \omega_\parallel = \omega_0(1-\tfrac{4}{3}\delta)^{1/2}, \quad \omega_0 = \mathring{\omega}_0(1-\tfrac{4}{3}\delta^2-\tfrac{16}{27}\delta^3)^{-1/6}, \tag{3}$$

where δ characterizes the deformation of the nuclear shape and $\mathring{\omega}_0$ its volume; $\hbar\mathring{\omega}_0 = 41.3A^{-1/3}$ (in MeV, A is the mass number of the nucleus).

We calculate the $|\chi_K^\tau\rangle$ eigenvectors of H_p, corresponding to the energies E_K^τ of the Nilsson orbits

$$|\chi_K^\tau\rangle = \sum_{l(j)} C_{lj}^{\tau K}|NlsjK\rangle , \tag{4}$$

where the shell number N is supposed to be a good quantum number, j and K refer to the angular momentum of the nucleon and its projection, $l = j \pm \frac{1}{2}$, and τ is the number of the Nilsson orbit. The summation in Eq. (4) extends over all possible (l, j) values in the shell.

The H_R part of the Hamiltonian is the quantum analog of the energy for a rigid body with an ellipsoidal symmetry rotating around its inertial center. It is written as usual

$$H_R = \frac{\hbar^2}{2\mathcal{J}}(J^2 + j^2 - 2\vec{I}\cdot\vec{j}), \tag{5}$$

where $\mathcal{J}$ ($\mathcal{J}_x = \mathcal{J}_y$) is the principal moment of inertia and $\vec{J}$ is the total spin of the nucleus. The eigenvectors of the Hamiltonian of Eq. (1) correspond to excited states with an energy E and are linear combinations ($K > 0$)

$$|EJM\rangle = \sum_{K\tau} D_{\tau K}^{EJ}|\tau JMK\rangle \tag{6}$$

of the eigenvectors of the rotational bands

$$|\tau JMK\rangle = \left(\frac{2J+1}{16\pi^2}\right)^{1/2}[\mathfrak{D}_{MK}^J|\chi_K^\tau\rangle + \mathcal{P}\mathfrak{D}_{M-K}^J|\chi_{-K}^\tau\rangle] \tag{7}$$

built on the intrinsic states $|\chi_K^\tau\rangle$ of the single nucleon defined above in Eq. (4). The phase factor $\mathcal{P}$ is determined from the symmetry of the nuclear shape and the definition of $|\chi_{-K}^\tau\rangle$, with

$$|\chi_{-K}^\tau\rangle = \sum_{l(j)}(-)^{j-1/2}C_{lj}^{\tau K}|Nlsj-K\rangle,$$

we have

$$\mathcal{P} = (-)^{J-1/2}.$$

The following assumptions will be made: (a) The pairing energy is independent of the Nilsson orbit occupied; (b) the proton (or neutron) core is inert when the last unpaired nucleon is a neutron (or a proton); (c) the mixing between rotational bands built on cores differing by two occupied states is negligible.

Thus, for each angular momentum J, the Hamiltonian of the nucleus, is diagonalized in the space spanned by the kets defined in Eq. (7). Then, the Nilsson orbits τ are those authorized by the Pauli principle for the outer nucleon (providing $K \leq J$). The calculation is performed separately for each following configuration of the core:

(i) "Particle" configuration with positive or negative parity, hereafter denoted as P^+ and P^-, respectively. For the cigar-shaped nuclei considered here, the deformations are positive, and the particle states corresponding to the Nilsson orbits of the $N = 0$, $N = 1$ shells and the Nilsson orbit 6 of the $N = 2$ shell are filled with two or four nucleons. The remaining particle states corresponding to the five other orbits in the $N = 2$ shell and the 10 orbits in the $N = 3$ shell are available for the outer nucleon. So the complete Hamiltonian is diagonalized here onto the subspace of the rotational bands [Eq. (7)] based on these 5 + 10 Nilsson orbits. We remark that the diagonalization can be carried out separately in each shell ($N = 2, 3$) because of their

different parity.

(ii) "Hole" configuration with positive parity (which will be denoted as H^+). A hole in the core is created on the Nilsson orbit 6. The orbit 7 is then filled with one or two pairs of nucleons and the subspace used when diagonalizing the Hamiltonian is that one spanned by the rotational bands based on the other five orbits of the $N=2$ shell. In addition, for the $\xi=13$ nuclei, the creation of a hole in Nilsson orbit 7 will be considered.

(iii) "Hole" configuration with negative parity (hereafter denoted as H^-). A hole is created in the core by lifting a nucleon to orbit 7 from orbit 4, to which is allotted the outer unpaired nucleon.

In order to locate the energies of the configurations with respect to one another, we calculate the total energy E_t of the "configuration heads"

$$E_t = \sum_{i=1}^{A-1} E_i + E_{\min}, \tag{8}$$

with

$$E_i = \tfrac{3}{4}E_K^\tau - \tfrac{1}{4}\langle C\vec{l}\cdot\vec{s} + D\,l^2\rangle_K^\tau . \tag{9}$$

The energy E_i $(i=\tau,K)$ is the contribution to the static energy of the i nucleon on the τ orbit, so the first term in Eq. (8) is the static energy of the core. The second term $E_{\min}$ in Eq. (8) is the minimum eigenvalue of the total Hamiltonian defined in Eq. (1): It represents the sum of the contribution of the unpaired nucleon to the static energy and of the core rotational energy, taking into account the correction due to the Coriolis coupling term.

The fitting parameters are only the deformation δ, the inverse moment of inertia $\hbar^2/2\mathcal{J}$, the coefficients $\kappa=-C/2\hbar\omega_0^0$, $\mu=2D/C$ of the $\vec{l}\cdot\vec{s}$, and l^2 terms in the Nilsson potential. They are adjusted with an automated search procedure to find the minimum of the standard deviation between the calculated and experimental energies.[5] Without assuming any rotational band identification, but discriminating among particle and hole states, we fitted only the levels with well-known spin and parity assignments. Mirror pair nuclei are discussed simultaneously and the energies to be fitted are then the averaged energies of the corresponding levels. For the sake of simplicity only the particle states with positive parity have been taken into account to determine the four parameters, which are then used in the energy calculation of the other configurations.

A first test of the wave functions so obtained is given by the spectroscopic factors for stripping reactions:

$$S_{ij}^{EJ} = \frac{2}{2J+1}\sum_{K\tau} |D_{\tau K}^{EJ} C_{ij}^{\tau K}|^2 , \tag{10}$$

with $j=J$ and $(-)^l$ equal to the parity of the state with E energy. These spectroscopic factors will cancel for residual positive-parity states with a spin $\geq\frac{7}{2}$ because these states belong to the $2s$-$1d$ shell only (the mixing of shells differing by $\Delta N=2$ is ignored). Except as concerns the band mixing between core configurations (i) and (ii), this first description of the energy levels uses a formulation similar to that of Malik and Scholz for the strong coupling model.[6] A detailed account of the calculations may be found in Ref. 7.

B. Second Description of the Energy Levels

In a second application of the Bohr-Mottelson and Nilsson model (which we shall denote from now on as TH.II), we introduce the following modifications:

(a) In the study of the single-nucleon Hamiltonian, the ϵ representation (see Appendix A, Ref. 2) is used. The pulsations in Eq. (2) are then

$$\omega_\perp = \omega_0(1+\tfrac{1}{3}\epsilon), \quad \omega_\parallel = \omega_0(1-\tfrac{2}{3}\epsilon),$$
$$\omega_0 = \omega_0^0\frac{\eta(\epsilon)\kappa}{\epsilon}, \tag{11}$$

with

$$\eta(\epsilon) = \frac{\epsilon}{\kappa}(1-\tfrac{1}{3}\epsilon^2-\tfrac{2}{27}\epsilon^3)^{-1/3}.$$

It should be remembered that $\delta\simeq\epsilon$, because the identification of Eqs. (3) and (11) leads to $\delta=\epsilon(1-\frac{1}{6}\epsilon)/(1+\frac{2}{9}\epsilon^2)$.

(b) For each configuration and rotational band defined by the set of occupied Nilsson orbits, we calculate the complete static energy of the nucleus

$$E_s = \sum_{i=1}^{A} E_i , \tag{12}$$

where E_i is known from Eq. (9), in which the bracket has been neglected. We found that the results obtained by minimizing E_s or E_t [Eq. (8)] are approximatively the same, but E_s is easier to handle. The comparison between the different E_s energies enables the various rotational bands to be located in energy with respect to one another. We note that these rotational bands have not the same deformation and are consequently not eigenvectors of the same Hamiltonian. However, these eigenvectors are then mixed by the Coriolis term as in TH.I.

(c) The energies of the particle states with negative parity are calculated apart from the orbit 14, i.e., the rotational bands are not mixed in the $1f$-$2p$ shell.

(d) The creation of a hole in the core in Nilsson orbit 2 is considered for the ^{21}Ne-^{21}Na mirror

pair.

(e) Finally, we search for one particular set of fitting parameters for each configuration, because different cores can reasonably generate different rotating potentials. Clearly, this process is justified only when enough experimental data are available. We used a simplex method[8,9] for the search procedure of the least-squares error of the calculated energies.

All complementary details are developed in Refs. 10 and 11.

C. Electromagnetic Properties

The calculations of electromagnetic properties have been carried out separately in TH.I and TH.II, but can be written both in the formalism by Rose and Brink.[12] We adopt their definitions of the transition rate T and reduced matrix elements B for radiative transitions of type σ (E, electric or M, magnetic), multipolarity λ, and connecting an initial nuclear state i to a final nuclear state f:

$$T_{if}(\sigma,\lambda) = \frac{2}{\hbar} k^{2\lambda+1} \frac{(\lambda+1)(2\lambda+1)}{\lambda[(2\lambda+1)!!]^2} \times \left| \langle E_i J_i \| T^{\sigma}_{\lambda} \| E_f J_f \rangle \right|^2 , \quad (13)$$

$$B_{if}(\sigma,\lambda) = \frac{2\lambda+1}{4\pi} \left| \langle E_i J_i \| T^{\sigma}_{\lambda} \| E_f J_f \rangle \right|^2 . \quad (14)$$

Here, E and J stand respectively for the energy and spin, while k is the wave number of the emitted photon. We regard the γ transition calculations as a test of the nuclear wave functions obtained after the mixing of rotational bands; thus k is everywhere set equal to the experimental value in order to avoid supplementary errors arising from the discrepancies between experimental and theoretical energies. In this work, we only deal with the $M1$-$E2$ transitions between P^+ states. Thus, separating the core and outer nucleon contributions, we get the following components of the useful T^{σ}_{λ} operators:

$$T^{M}_{1\mu} = \mu_N \{ g_R J_\mu + (g_l - g_R) j_\nu + (g_s - g_l) S_\nu \} \quad (15)$$

written in the laboratory system, where $\mu_N = e\hbar/2mc$ is the nuclear magneton, and g_R, g_l, and g_s are the core-, orbital-, and spin-gyromagnetic ratios, respectively. We choose $g_R = Z/A$ (Z atomic number, A mass number) and for g_l and g_s values those of the single (unbound) nucleon

$$T^{E}_{2\mu} = e \left[\tfrac{1}{2} Q_i \, \delta_{\nu 0} + (g_l + Z_c/A^2)(\tfrac{4}{5}\pi)^{1/2} r^2 Y^{\nu}_2(\theta,\varphi) \right] . \quad (16)$$

Q_i is the intrinsic quadrupole moment operator of the core with Z_c protons. This operator gives the matrix element of $T^{E}_{2\mu}$ a contribution $\frac{4}{5} Z_c R_0 \delta (1 + \frac{2}{3}\delta + \cdots)$, for example, in the δ representation, where $R_0 = r_0 A^{1/3}$ is the charge radius of the nucleus and the values chosen for r_0 are those of Ref. 13. In TH.II, we attribute to all states of a given rotational band the Q_i operator corresponding to the equilibrium deformation and correction terms analogous to those already derived in the asymptotic basis[8] which are introduced in the expressions of the electromagnetic transition operators.

Finally, the magnetic dipole moment μ and electric quadrupole moment Q for the state $|EJ\rangle$ are:

$$\mu = [J/(J+1)]^{1/2} \langle EJ \| T^{M}_{1} \| EJ \rangle , \quad (17)$$

$$Q = 2 \left[\frac{J(2J-1)}{(J+1)(2J+3)} \right]^{1/2} \langle EJ \| T^{E}_{2} \| EJ \rangle . \quad (18)$$

III. $\xi = 11$ NUCLEI: RESULTS

A. ^{19}O Nucleus (Refs. 14 to 20)

A limited amount of experimental information exists regarding the ^{19}O nucleus, since ambiguities in spin assignments appear from the third excited level (see Fig. 1). The results of the optimization in both TH.I (Table I) and TH.II (Table II) are compared to the experimental data on Fig. 1 where we report the experimental sequence of the five levels we tried to reproduce.

The predictions of both methods are quite consistent for the P^+ states. The theoretical energies of the optimized levels (except for the $\frac{7}{2}^+$) are in good agreement with the experiment. Furthermore, it seems possible to make a correspondence between (i) the second theoretical $\frac{5}{2}^+$ level and the experimental $\frac{5}{2}^+$ level at 3.16 MeV, (ii) the second theoretical $\frac{3}{2}^+$ level and the 3.07-MeV experimental level with the spin assignment $\leqslant \frac{7}{2}$. The main difficulty encountered is the presence of the $\frac{7}{2}^+$ level at an energy less than 1.5 MeV in both methods of calculation: This state is therefore too low to yield a satisfactory interpretation of the 2.37-MeV experimental state which has been optimized with $J^{\pi} = \frac{7}{2}^+$ assignment. We were unable to bring up to this level in the framework of the Nilsson model. Other trials with different

TABLE I. Fitting parameters used in the first theoretical description (TH. I) of the $\xi = 11$ and $\xi = 13$ nuclei.

	δ_I	μ_I	κ_I	$\hbar^2/2\mathcal{I}_I$ (keV)
^{19}O	0.159	0.0046	0.078	294
^{21}Ne-^{21}Na	0.242	0.0675	0.089	250
^{23}Na-^{23}Mg	0.325	0.106	0.080	205
^{23}Ne	0.246	0.082	0.114	234
^{25}Mg-^{25}Al	0.239	0.173	0.088	215
^{27}Al-^{27}Si	0.164	0.254	0.074	320

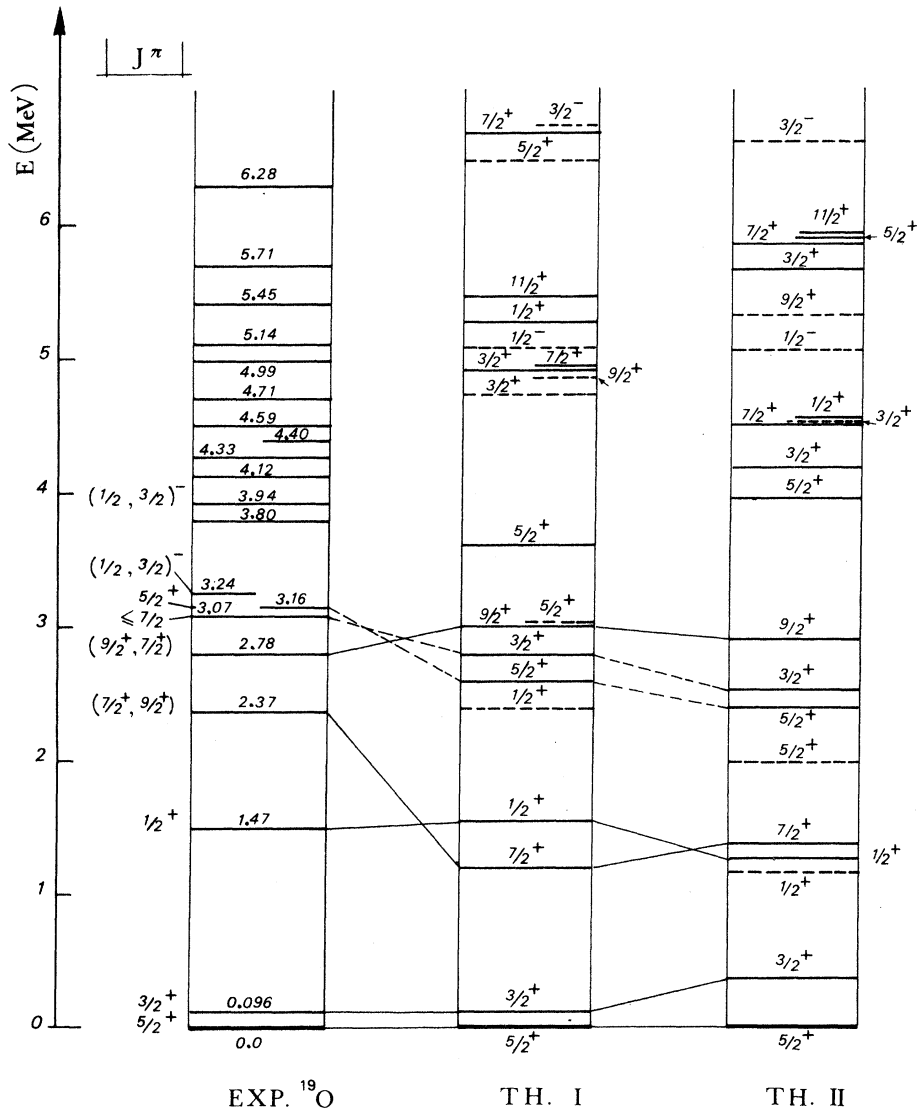

FIG. 1. Energy levels of ^{19}O. The experimental data (EXP) are taken from Refs. 14 and 15. The theoretical results (TH.I) and (TH.II) respectively refer to the first and second descriptions in the framework of the Bohr-Mottelson and Nilsson models (see the text). The dotted levels in the theoretical spectra correspond to hole states and the others to particle states. The solid lines join the levels we take into account in the minimization of the least-squares error of the calculated energies. The dashed lines show prospective identification of some nonoptimized levels. The fitting parameters and the deformations are given in Tables I and II.

TABLE II. Equilibrium deformations $\eta(\epsilon)$ used in the second theoretical description (TH.II) of ^{19}O. The fitting parameters are $\mu_{II}=0.013$, $\kappa_{II}=0.081$, and $\hbar^2/2\mathcal{I}=310$ keV for all rotational bands.

Core	With hole			Without hole				
Configuration of the core	$(134)^4(267)^2$	$(123)^4(467)^2$	$(1234)^4(7)^2$	$(1234)^4(6)^2$				
Band based on orbit:	2	4	6	7	5	9	11	8
$\eta(\epsilon)$	3.4	3.4	1.7	2.8	1.5	2.7	2.2	1.7

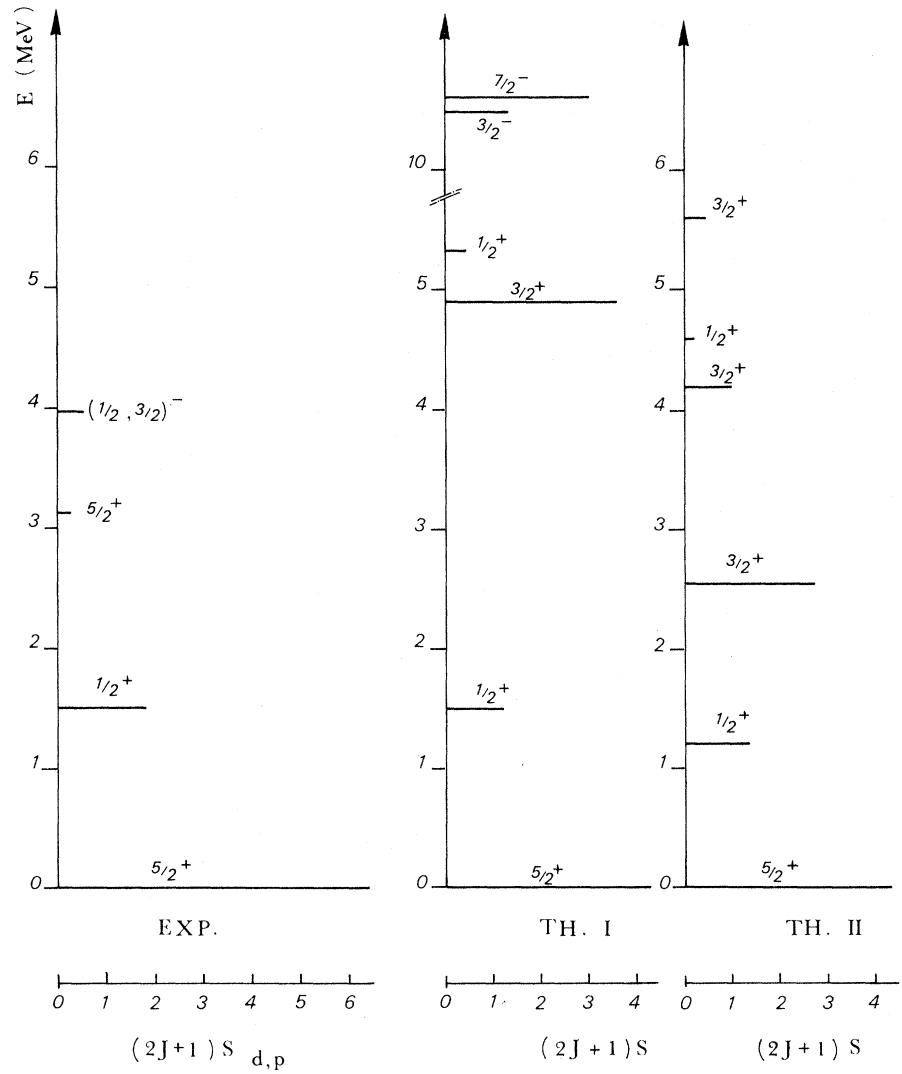

FIG. 2. Spectroscopic factors of ^{19}O. The experimental values are those of the $^{18}O(d,p)$ reaction (Ref. 15).

sequences of levels to be optimized have been made (e.g., taking into account new $\frac{9}{2}^+$, $\frac{7}{2}^+$ assignments for the 2.37- and 2.78-MeV levels, respectively[14]), they do not yield noticeable improvement for the $\frac{7}{2}^+$ theoretical level and perturb the low-lying spectrum.

The calculations for the other configurations energies give:

(a) The P^- states above 10.5 MeV ($\frac{3}{2}^-$) in TH.I. They cannot explain correctly the $(\frac{1}{2}, \frac{3}{2})^-$, 3.94-MeV level identified[15] as a particle state from the stripping reaction $^{18}O(d, p)$. They are not calculated in TH.II.

(b) The H^+ states appearing at about 2.2 MeV in TH.I and 1.2 MeV in TH.II. The shift between these energies could be explained by the different methods used for placing the configuration heads (see Sec. II). One cannot identify corresponding H^+ levels in the experimental spectrum.

(c) The H^- states above 5 MeV ($\frac{1}{2}^-$) in both methods These are too high with respect to the experimental $(\frac{1}{2}, \frac{3}{2})^-$, 3.24-MeV level, which is a prospective

TABLE III. Static moments of the ground state of the $\xi = 11$ and $\xi = 13$ nuclei. The electric quadrupole moments Q are in e fm^2, the magnetic dipole moments μ in nuclear magnetons.

Nucleus	Q_{EXP}	$Q_{TH.I}$	$Q_{TH.II}$	μ_{EXP}	$\mu_{TH.I}$	$\mu_{TH.II}$
^{19}O	···	1.43	0.745	···	−1.41	−1.44
^{21}Ne	9.1	5.38	8.41	−0.66	−0.86	−0.92
^{21}Na	···	6.68	10.2	2.386	2.56	2.63
^{23}Na	10.1 ± 0.1	9.33	10.1	2.21	2.69	2.64
^{23}Mg	···	9.67	10.0	···	−0.97	−0.93
^{23}Ne	···	10.2	10.1	···	−1.10	−1.10
^{25}Mg	22	12.86	13.9	−0.885	−1.09	−1.09
^{25}Al	···	10.82	12.3	···	3.85	3.84
^{27}Al	15.2	6.09	4.58	3.638	3.86	3.85
^{27}Si	···	9.51	7.48	···	−1.10	−1.09

hole state from stripping reaction.[15]

The spectroscopic factors of the P^+ states below 4 MeV are in good qualitative agreement with the $^{18}O(d,p)$ reaction in TH.I (see Fig. 2). The agreement is correct too for the first P^- state, but we saw above that this level appears theoretically at a far too high energy. In TH.II, the spectroscopic factor of the $\frac{3}{2}^+$ 2.55-MeV level is much too important, contrary to TH.I and to the experiment.

No experimental information is available on the static moments of the ground state. The theoretical values are given in Table III. It is apparent that the two calculated values of the electric quadrupole moment differ by a factor of 2. This can be justified by the relatively small value $\eta(\epsilon) = 1.5$ used for the deformation of the ground state in TH.II (See Tables I and II to compare this value to others), which lower the Q_i term in Eq. (16) in spite of the important mixing of the rotational band based on the orbit 7. On the contrary, the two calculated values of the magnetic dipole moment are quite consistent.

The $E2$ and $M1$ radiative decays of the P^+ are compared to the experimental data on Fig. 3. No model-predicted lifetime is in quantitative agreement with the experiment, except for the first excited level in TH.II. It is in these results that the discrepancies between TH.I and TH.II are most important: We have checked the sensitivity of the lifetime values to small deviations of the parameters. The branching ratios given by both models are quite consistent with the experiment, except for the 2.78-MeV level, interpreted with a $\frac{9}{2}^+$ assignment, which has a theoretically noticeable branch towards the 2.37-MeV level interpreted with a $\frac{7}{2}^+$ assignment. The mixing ratios are in

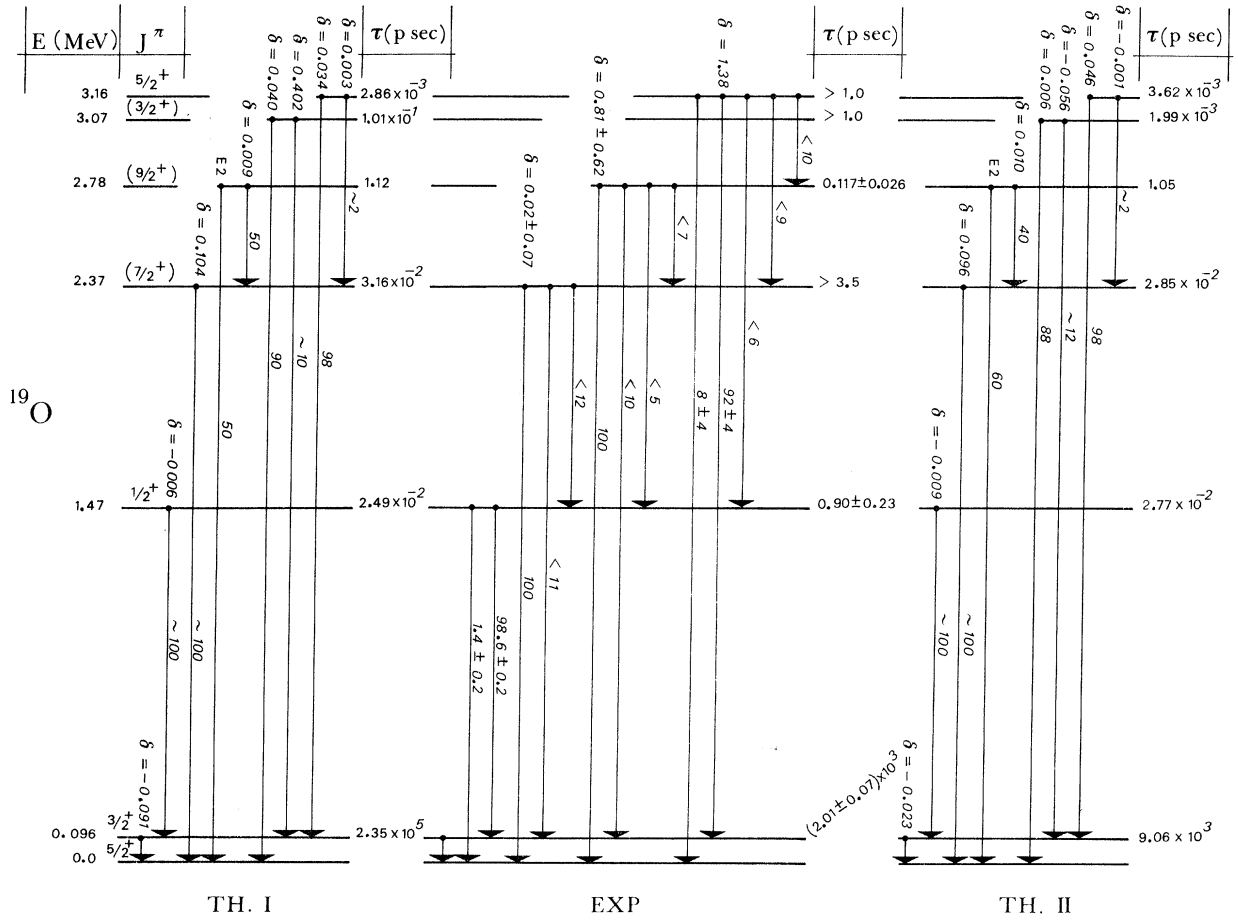

FIG. 3. Electromagnetic properties of the P^+ states of ^{19}O. The experimental lifetimes τ are from Ref. 16 (first excited state), Ref. 14 (second to fourth), and Ref. 17; the branching ratios are from Ref. 18 (1.47-MeV state) and Ref. 19, the mixing ratios δ from Ref. 14. The theoretical values (TH.I, TH.II) are computed with the experimental energies, and the wave functions and parameters leading to the theoretical spectra of Fig. 1, without any inclusion of other fitting parameters. For the mixing ratios δ, only $\delta(E2/M1)$ is calculated. The choice of the more probable J^π assignment for some levels is pointed out with parentheses.

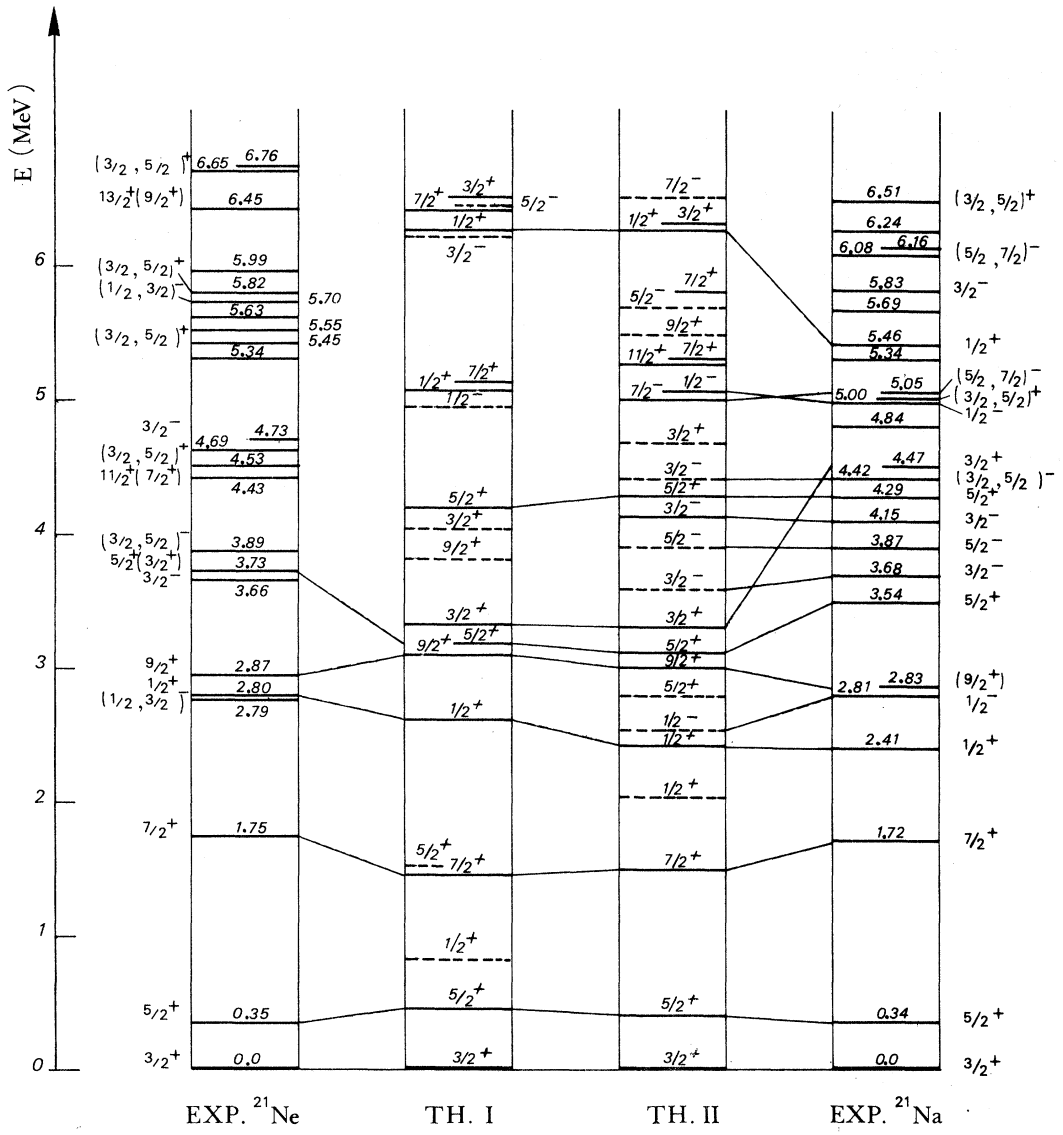

FIG. 4. Energy levels of ^{21}Ne and ^{21}Na. The experimental data of ^{21}Ne are taken from Ref. 21 except for 4.43- and 6.45-MeV levels (Ref. 22). Those of ^{21}Na are taken from Ref. 23. The same notations as in Fig. 1 are used. The fitting parameters and the equilibrium deformations are given in Tables I and IV.

TABLE IV. Equilibrium deformations $\eta(\epsilon)$ and fitting parameters used in the second theoretical description (TH. II) of the ^{21}Ne-^{21}Na mirror pair. The parameter κ_{II} is 0.115 for all bands (see the text). The $\eta(\epsilon)$ value for the orbit 14 has been readjusted.

Core	With hole			Without hole					
Configuration of the core	$(1346)^4(27)^2$	$(1236)^4(47)^2$	$(1234)^4(67)^2$	$(12346)^4$					
Band based on orbit:	2	4	6	7	9	5	11	8	14
$\eta(\epsilon)$	3.5	3.5	2.5	3.2	3.2	2.5	2.8	2.6	3.2
μ_{II}	0.10			0.05					
$\hbar^2/2\mathcal{J}$ (keV)	2.60	221		253					150

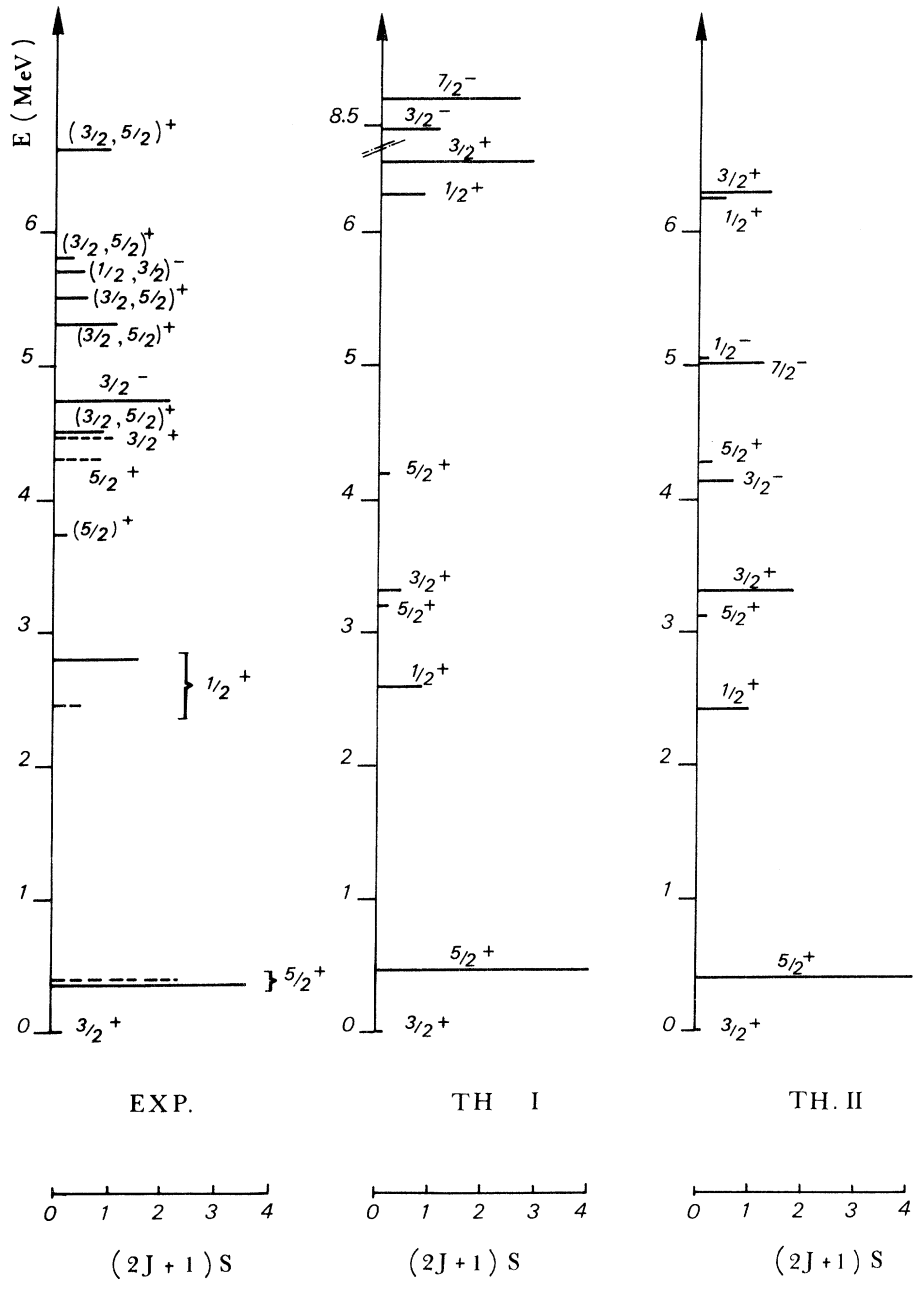

FIG. 5. Spectroscopic factors of ^{21}Ne and ^{21}Na. The experimental values correspond to the reactions ^{20}Ne(d,p) (Ref. 21—(solid lines) and ^{20}Ne(d,n) (Refs. 24, 25)—(dashed lines).

qualitative agreement with the experimental decays of the 2.37- and 3.16-MeV levels. The $\frac{9}{2}^+$ assignment to the 2.78-MeV level forbids the $M1$ multipole in the branch towards the ground state. Thus, we cannot discuss the experimental value[14] of the mixing ratio for the 2.78 MeV → 0.0 MeV transition because we do not deal with the $M3$ multipole. The $\frac{7}{2}^+$ level at about 1.5-MeV energy in the theoretical spectrum leads to discrepancies with the experimental transition data and cannot account for $\frac{9}{2}^+$ and $\frac{7}{2}^+$ assignment to 2.37- and 2.78-MeV levels. In a recent study,[20] the hypothesis of axial asymmetry has yielded noticeable improvement for the ^{19}O nucleus.

B. ^{21}Ne and ^{21}Na Nuclei (Refs. 21 to 29)

Figure 4 compares the model-predicted results and the experimental data on ^{21}Ne-^{21}Na mirror

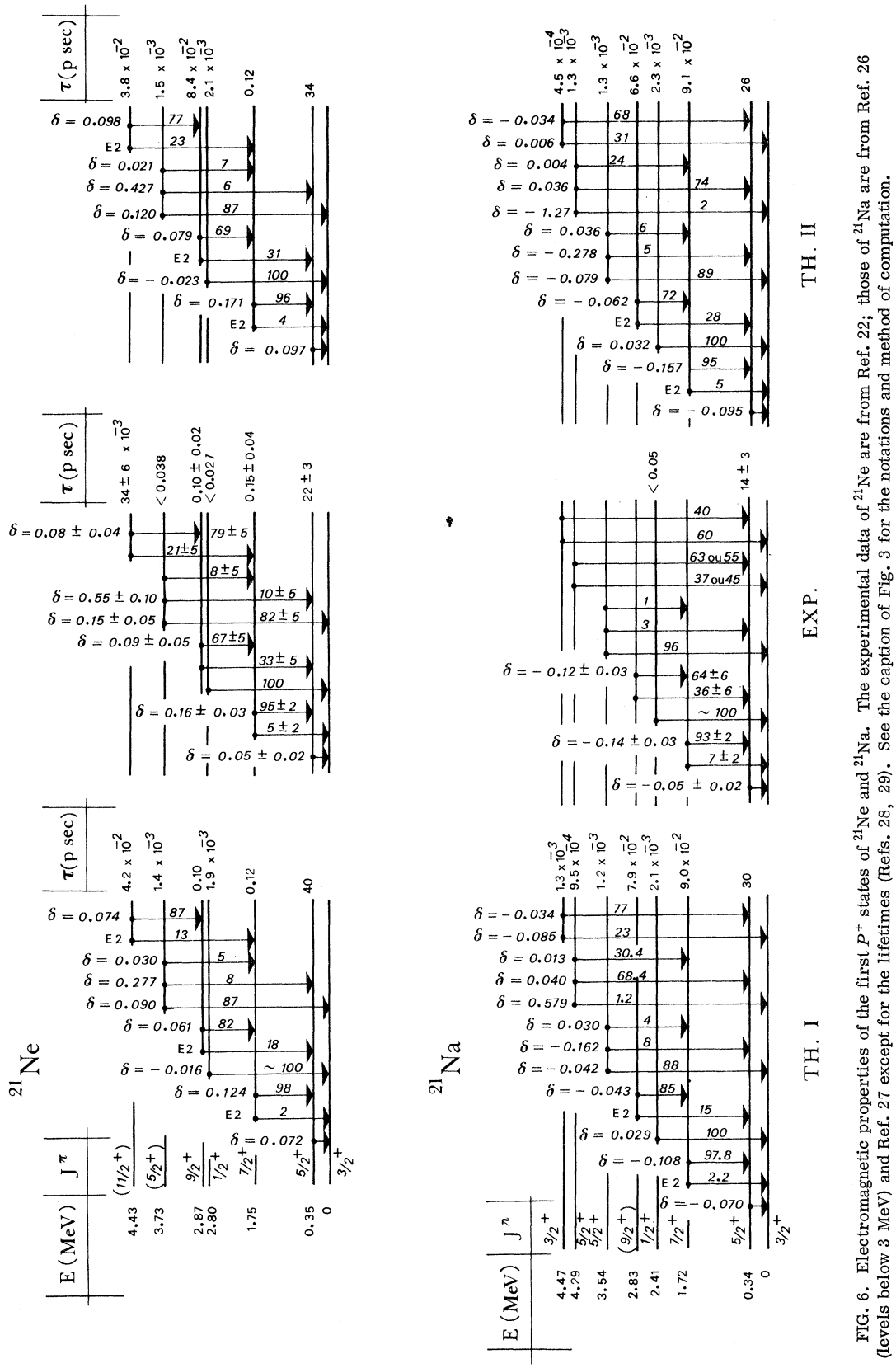

FIG. 6. Electromagnetic properties of the first P^+ states of ^{21}Ne and ^{21}Na. The experimental data of ^{21}Ne are from Ref. 22; those of ^{21}Na are from Ref. 26 (levels below 3 MeV) and Ref. 27 except for the lifetimes (Refs. 28, 29). See the caption of Fig. 3 for the notations and method of computation.

pair spectra. Some data have already been given in Refs. 10 and 23.

Both nuclei have been heavily studied, so nine P^+ levels can be included in the energy sequence to be optimized. The TH.I and TH.II spectra are quite consistent and in good agreement with experiment, except for the second $\frac{3}{2}^+$ level (at 4.46-MeV energy) and the second $\frac{1}{2}^+$ level (at 5.46-MeV energy) which are placed respectively too low and too high by the model.

The P^- states appear at about 8.5-MeV energy in the TH.I spectrum. This energy is too high compared with those of 4.73- and 5.69-MeV states in ^{21}Ne [with $\frac{3}{2}^-$ and $(\frac{1}{2}, \frac{3}{2})^-$ assignments, respectively] and those of 4.15-, 4.98-, and 5.03-MeV states in ^{21}Na [with $\frac{3}{2}^-$, $\frac{1}{2}^-$, $(\frac{5}{2}, \frac{7}{2})^-$ assignments, respectively] which can be considered as particle states.[21,23] For that reason, in TH.II, the deformation and the moment of inertia have been fitted so as to reproduce the P^- states of ^{21}Na (see Table IV). This modest supplementary parametrization leads to an excellent agreement with the three experimental levels.

The H^+ states are calculated with the same parameters as the P^+ states. The same general conclusions as for ^{19}O can be taken again, even if one tentatively interprets the $\frac{5}{2}^+$, 3.54-MeV state in ^{21}Na as a hole state in orbit 6 because of its small spectroscopic factor (see Fig. 4): With this interpretation, the other theoretical H^+ states have

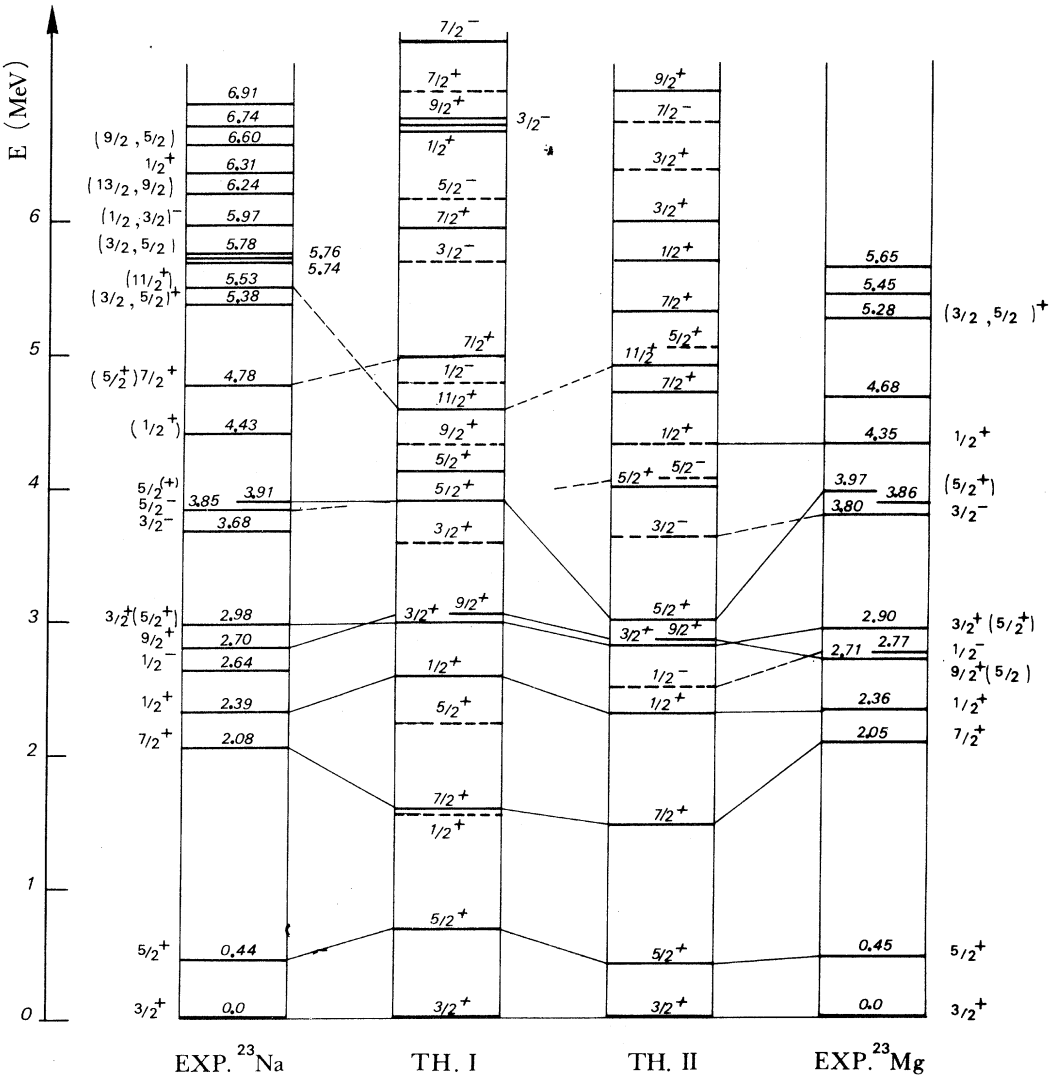

FIG. 7. Energy levels of ^{23}Na and ^{23}Mg. The experimental data are from Ref. 30 for ^{23}Na and from Ref. 31 for ^{23}Mg, except for the 2.05- and 2.77-MeV levels (Ref. 32). The same notations as in Fig. 1 are used. The fitting parameters and the equilibrium deformations are given in Tables I and V.

no corresponding prospective experimental states presently known at such a low energy.

The TH.I model prediction concerning the H^- state is a sequence $\frac{1}{2}^-$, $\frac{3}{2}^-$, $\frac{5}{2}^-$, placed 2.5 MeV above the possible corresponding experimental sequences[21,23]: 2.79 and 3.66 MeV in ^{21}Ne and 2.81, 3.68, and 3.87 MeV in ^{21}Na. A good agreement is obtained in TH.II by adjusting the inertia parameter alone (see Table IV).

The theoretical spectroscopic factors of the ^{21}Ne-^{21}Na mirror pair and those of ^{20}Ne(d,p) and ^{20}Ne(d,n) reactions are shown on Fig. 5. The consistency is good for the first six P^+ states observed in stripping, in spite of the wrong energy of the second $\frac{3}{2}^+$ state. The spectroscopic factors of negative-parity states are only semiquantitatively represented in TH.II where these states have correct energies. In TH.I, as in the ^{19}O investigation, we notice that there is an important theoretical spectroscopic factor for the $\frac{7}{2}^-$ state.

The calculated static moments of the ground state are compared to the experiment in Table III. As for ^{19}O, the two model-predicted values of the magnetic dipole moment (μ) are consistent, though those of the electric dipole moment (Q) are different. TH.I gives the best agreement with the observed μ value and TH.II with the observed Q value. It does not seem possible to improve the Q value in TH.I by introducing an effective charge as fitting parameter without perturbing some transition rates; it does not seem possible too, to improve the μ value of ^{21}Ne in TH.II by using $g_R \neq Z/A$ for the gyromagnetic factor without perturbing the μ value of ^{21}Na [10] and some transition rates.

The model-predicted transition rates of the first P^+ states are consistent in TH.I and TH.II (see Fig. 6), the most important discrepancy appearing in the lifetime of the first excited level [40 ps in TH.I, 34 ps in TH.II, and (22 ± 3) ps in the experiment[22] on ^{21}Ne for example]. The consistency with experiment is satisfying for the $A = 21$ mirror pair, with a possible exception for the branching ratios of the $\frac{9}{2}^+$ state in TH.I (the predictions of TH.II are better). Additionally, the agreement with experiment is correct for the 4.43-MeV level in ^{21}Ne with $(\frac{11}{2}^+)$ assignment. On the contrary, the branching ratios of the last two levels considered here in ^{21}Na (4.29 and 4.47 MeV) are at variance with the experimental data (let us remark that the 4.47-MeV level has an incorrect theoretical energy, see Fig. 4).

C. ^{23}Na and ^{23}Mg Nuclei (Refs. 30 to 37)

Figure 7 shows a comparison between the observed and model-predicted spectra of the ^{23}Na-^{23}Mg mirror pair. The seven P^+ states included in the sequence to be optimized are well reproduced by both TH.I and TH.II methods. Furthermore, one could possibly interpret the 4.78- and 5.53-MeV levels in ^{23}Na respectively as a second $\frac{7}{2}^+$ state and a first $\frac{11}{2}^+$ state. However, another sequence $(\frac{5}{2}^+, \frac{7}{2}^+, \frac{9}{2}^+)$ appears in the theoretical spectra, corresponding to a rotational band based on orbit 5, before the band mixing. This sequence has no well-known experimental counterpart, since it starts from a 3-MeV energy in TH.II and 1 MeV higher in TH.I where they are consequently less disturbing.

The P^- states appear at 6.7 MeV in TH.I. Two experimental negative-parity states do exist at 5.97- and 6.91-MeV energies, but because of the lack of experimental information concerning these levels, they have not been calculated in TH.II.

As concerns the H^+ states calculated in TH.I with the same parameters as the P^+ states, their spectrum starts from 1.5-MeV energy. This is too low an energy to give a satisfactory interpretation of the second experimental $\frac{1}{2}^+$, 4.43-MeV level in ^{23}Na [33] (and 4.35-MeV level in ^{23}Mg). It has been possible to interpret this level in TH.II

TABLE V. Equilibrium deformations $\eta(\epsilon)$ and fitting parameters used in the second theoretical description (TH. II) of the ^{23}Na-^{23}Mg mirror pair. The parameter κ_{II} is 0.10 for all bands.

Core	With hole			Without hole				
Configuration of the core	$(13467)^4(2)^2$	$(12367)^4(4)^2$	$(12347)^4(6)^2$	$(12346)^4(7)^2$				
Band based on orbit:	2	4	6	7	5	9	11	8
$\eta(\epsilon)$	3.9	3.9	2.9	3.6	2.9	3.7	3.0	2.9
μ_{II}	0.175		0.089	0.175				
$\hbar^2/2\mathcal{J}_{II}$ (keV)	235		217	235				

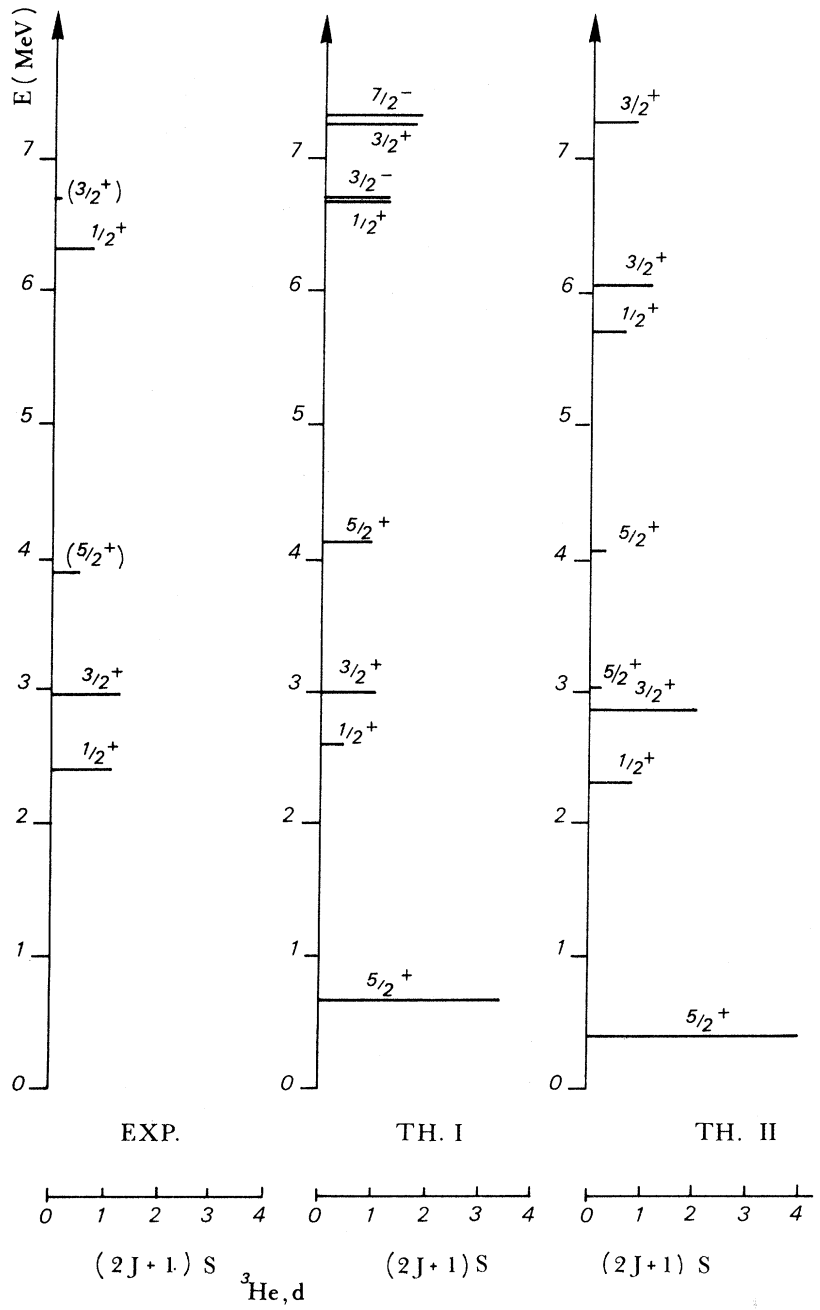

FIG. 8. Spectroscopic factors of ^{23}Na and ^{23}Mg. The experimental values correspond to the ^{22}Ne(^{3}He, d) reaction (Ref. 33).

with new values of κ and μ parameters (see Table V), but with the equilibrium deformation and the same value of $\hbar^2/2\mathcal{I}$ as for the P^+ states. The second theoretical H^+ level has a 5-MeV energy and might be related to the experimental $(\frac{3}{2}, \frac{5}{2})^+$, 5.38-MeV level of ^{23}Na observed in the ^{24}Mg(p, $2p$) reaction.[34]

The calculation of the energies of the H^- states in TH.I gives the sequence $\frac{1}{2}^-$, $\frac{3}{2}^-$, $\frac{5}{2}^-$ placed at a 2.1-MeV energy above the suggested experimental H^- sequences[33]: 2.64, 3.68, and 3.85 MeV in ^{23}Na, and 2.77 and 3.80 MeV in ^{23}Mg. These levels are placed quite well in TH.II without any adjustment of the parameters.

The theoretical spectroscopic factors of the ^{23}Na-^{23}Mg mirror pair are in good agreement with those of the ^{22}Ne(^{3}He, d) reaction,[33] with the possible exception of the first $\frac{5}{2}^+$ excited state for which no experimental measurement seems to have been performed (Fig. 8).

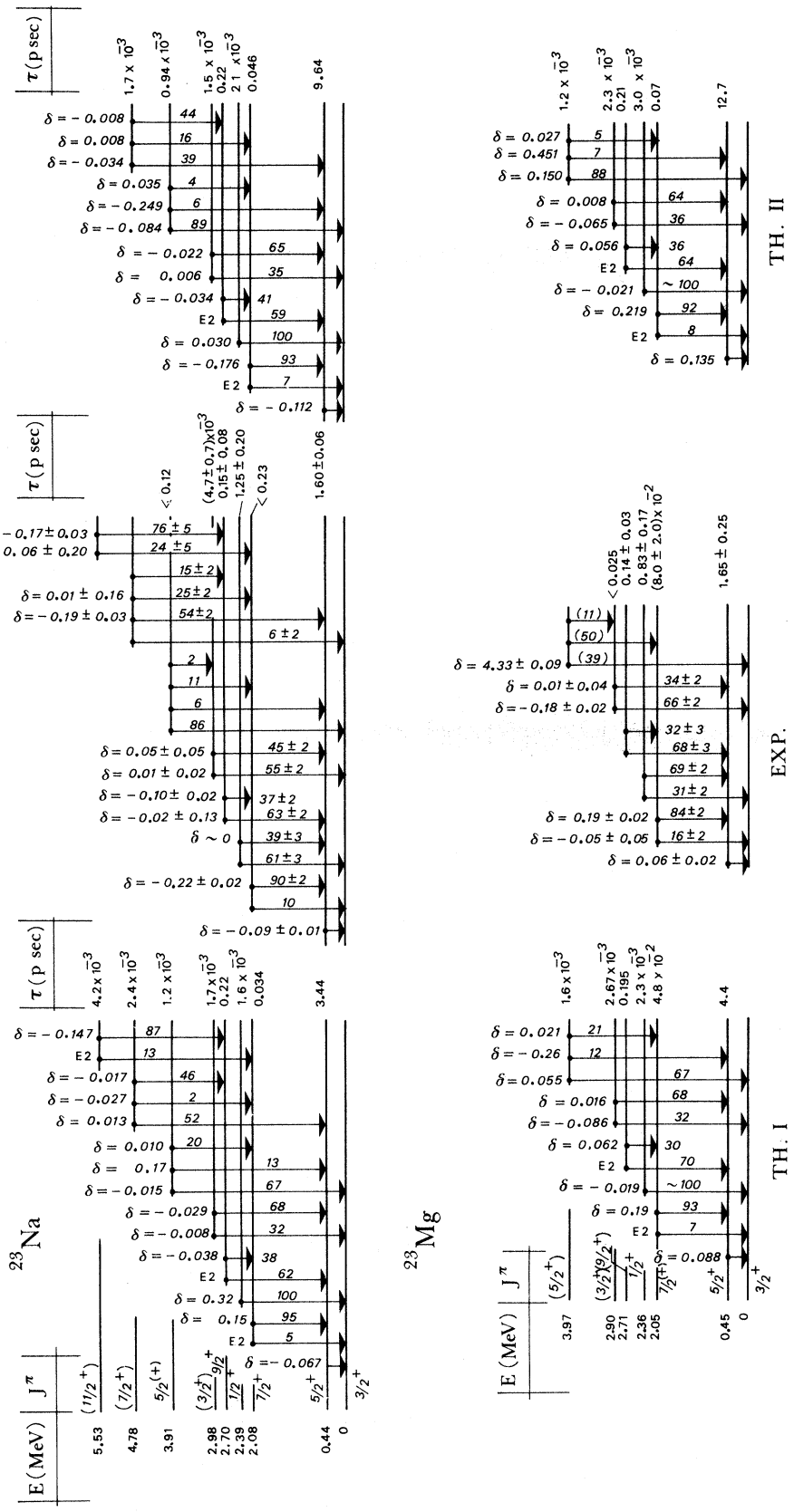

FIG. 9. Electromagnetic properties of the first P^+ states of ^{23}Na and ^{23}Mg. The experimental branching and mixing ratios are taken from Refs. 30 and 31 for ^{23}Na and ^{23}Mg respectively; the lifetimes are from Ref. 35 for ^{23}Na and from Ref. 32 for ^{23}Mg. See the caption of Fig. 3 for the notations and method of computation.

The static moments of the ground state are compared to the experimental data for ^{23}Na in Table III. The consistency is good in both TH.I and TH.II.

The radiative decays ($M1, E2$) of the first P^+ states are compared to experiment in Fig. 9. As for the other nuclei, there is a discrepancy between the predictions of TH.I and TH.II for the lifetime of the first excited state; but this time, TH.I gives the best result [$\tau_I = 3.44$ ps, $\tau_{II} = 9.64$ ps, $\tau_{exp} = (1.60 \pm 0.06$ ps) for ^{23}Na for example]. The other lifetimes are quite consistent in both calculations and in good agreement with the experimental values except for the third excited 2.39- and 2.36-MeV states in ^{23}Na and ^{23}Mg, respectively. On the other hand, these levels have no theoretical radiative branch to the first excited state; this is in contradiction with experiment. A qualitative agreement between the experiment and the calculations (TH.I and TH.II) is found for the branching and mixing ratios even for the 5.53-MeV level in ^{23}Na with the prospective $\frac{11}{2}^+$ assignment.

Our conclusions are in agreement with those of other authors, i.e., (i) there are difficulties[31, 36, 37] for the first $\frac{1}{2}^+$ excited state and to a less extent for the second $\frac{3}{2}^+$ state (at 2.98- and 2.90-MeV energy in ^{23}Na and ^{23}Mg, respectively), and (ii)

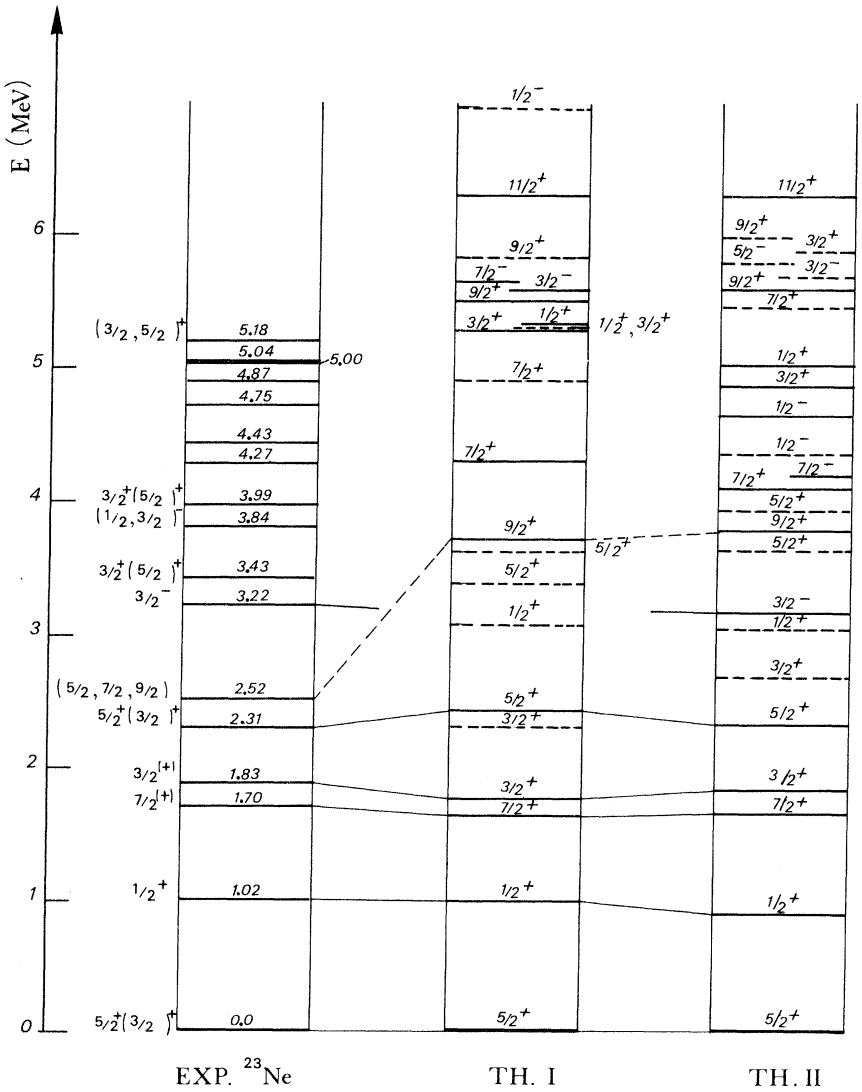

FIG. 10. Energy levels of ^{23}Ne. The experimental data are taken mainly from Ref. 21. In case of spin and parity ambiguity assignment, Ref. 38 (1.70- and 2.52-MeV states), Ref. 39 (2.31-, 2.43-, and 3.99-MeV states), and Ref. 40 (3.43- and 3.99-MeV states) are taken into account. The values of the fitting parameters and of the equilibrium deformations are given in Tables I and VI.

more satisfactory results[30] are obtained concerning the levels which correspond to the rotational band based on the ground state before the band mixing.

IV. $\xi = 13$ NUCLEI: RESULTS

A. ^{23}Ne Nucleus (Refs. 21, 38 to 44)

Though ^{23}Ne is a nucleus lying in an intensively studied region of the lower $2s$-$1d$ shell, spin assignment ambiguities exist from (and above) the fourth excited level (see Fig. 10).

As regards the positive-parity particle states (P^+), the two methods of calculation (TH.I and TH.II) developed in the preceding paper reproduce quite well the first five levels introduced in the energy sequence to be fitted. The first theoretical level with $\frac{9}{2}^+$ assignment may correspond to the 2.52-MeV experimental level,[41] if necessary. However, above 3.-MeV experimental energy, the disagreement between the experiment and the theoretical results is quite important since no

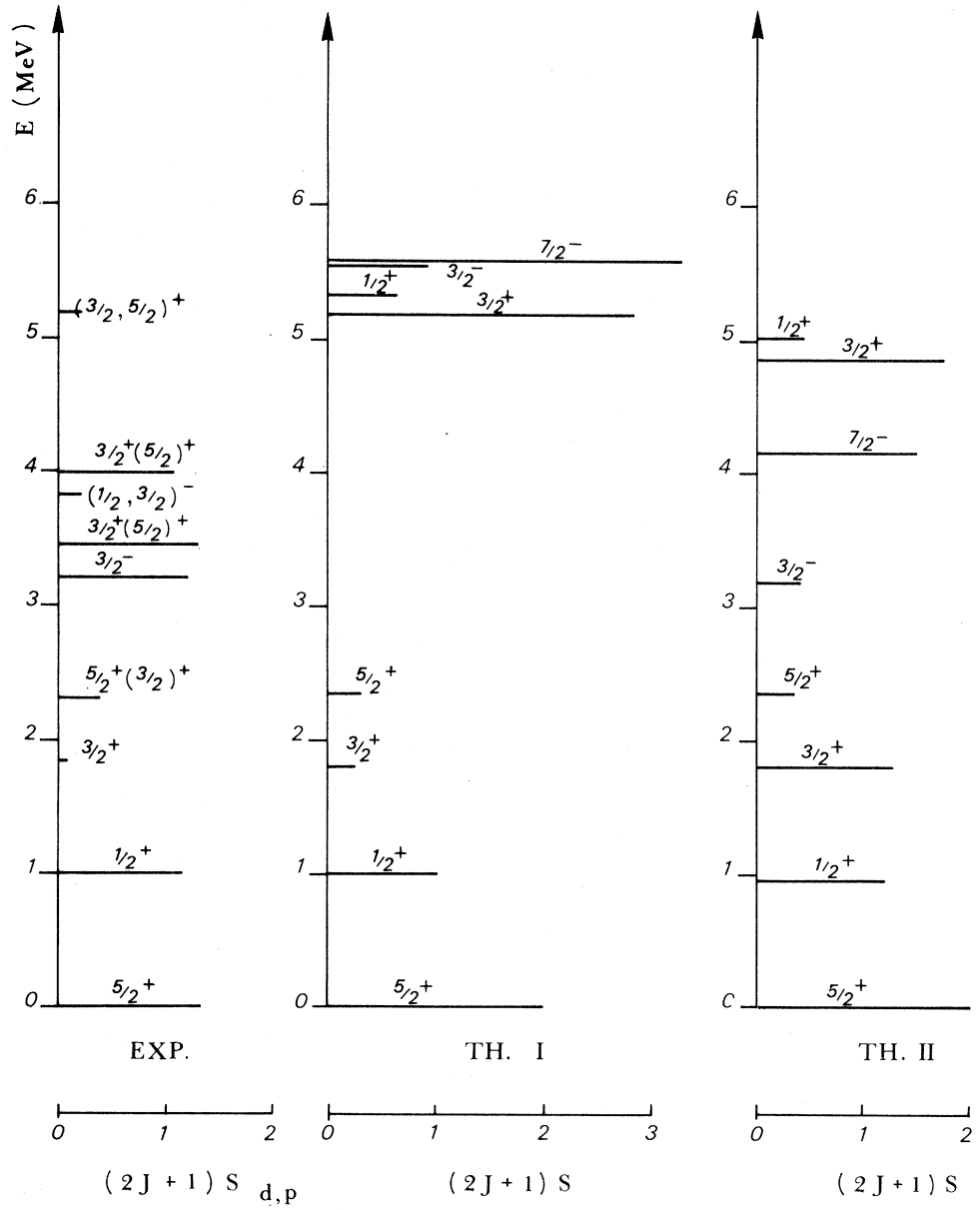

FIG. 11. Spectroscopic factors of ^{23}Ne. The experimental values are those of the ^{22}Ne(d,p) reaction (we took the average of the values given in Refs. 21, 38, 39, 43).

TABLE VI. Equilibrium deformations $\eta(\epsilon)$ used in the second method of calculation (TH. II) for ^{23}Ne [the value of $\eta(\epsilon)$ for the orbit 14 is not the equilibrium deformation, but is readjusted to fit experiment]. The fitting parameters are $\mu_{II}=0.095$, $\kappa_{II}=0.139$, and $\hbar^2/2\mathcal{J}_{II}=235$ keV for all the orbits, except for the orbit 14 ($\hbar^2/2\mathcal{J}_{II}=200$ keV).

Core	With hole				Without hole				
Configuration of the core	$(1346)^4(257)^2$	$(1236)^4(457)^2$	$(1234)^4(567)^2$	$(12346)^4(5)^2$	$(12346)^4(7)^2$				
Band based on the Nilsson orbit:	2	4	6	7	5	9	11	8	14
$\eta(\epsilon)$	1.6	1.5	0.7	1.3	1.9	2.4	2.2	2.0	2.2

other theoretical $\frac{3}{2}^+$ or $\frac{5}{2}^+$ state is found below 5 MeV to interpret the 3.43- and 3.99-MeV experimental states with $\frac{3}{2}^+$, $(\frac{5}{2}^+)$ assignment.

The calculations for the other configuration energies give:

(i) Negative-parity particle states (P^-) at about 5.5 MeV in TH.I. These states are at too high an energy to account for the 3.22- and 3.84-MeV states correctly. These can be identified as particle states because of their spectroscopic factor in (d, p) stripping reaction[42] (see Fig. 11). In TH.II, choosing the deformation $\eta(\epsilon)$ (see Table VI) and the inverse moment of inertia ($\hbar^2/2\mathcal{J}$) as new fitting parameters, it is possible to adjust a theoretical $\frac{3}{2}^-$ level close to the experimental 3.22-MeV level. The associated theoretical $\frac{1}{2}^-$ level is then 0.8 MeV above the experimental 3.84-MeV level with $(\frac{1}{2}, \frac{3}{2})^-$ assignment.

(ii) Positive-parity hole states (H^+) appearing between 2 and 3 MeV in both calculations. The number of these H^+ states is more important than in the case of $\xi=11$ nuclei. This is due to the additional possibility of creating a hole in the core in Nilsson orbit 7. It seems difficult to interpret the 1.83-MeV experimental state as a hole state because of its rather small spectroscopic factor (see Fig. 11); this would leave the first theoretical $\frac{3}{2}^+$ P^+ state without any reasonable corresponding state in the experimental spectrum.

(iii) Negative-parity hole states (H^-) lying above 7 MeV in TH.I and above 4.3 MeV in TH.II. The present experimental information concerning these H^- states seems to be too limited to entail a discussion.

The theoretical spectroscopic factors are consistent in TH.I and TH.II and in good agreement with experiment for the states with fitted energy (see Fig. 11). Several states above 4 MeV have an important theoretical spectroscopic factor (this fact has been noted above, in particular, for the $\frac{7}{2}^-$ state of the $\xi=11$ nuclei).

The experimental static moments of the ground state have not been measured. The theoretical values are quite similar in both methods of calculation (see Table III). The $E2, M1$ theoretical deexcitations of the first P^+ states are compared to experiment on Fig. 12. The predictions of both versions of the model are in good agreement with respect to one another, and in semiqualitative agreement with experiment. The difficulties are: (i) two model-predicted branchings: (1.83 MeV, $\frac{3}{2}^+ \rightarrow$ 1.02 MeV, $\frac{1}{2}^+$) and [2.52 MeV, $(\frac{9}{2})^+ \rightarrow$ 1.70 MeV, $\frac{7}{2}^+$] which are not experimentally measured, and (ii) an abnormal theoretical lifetime of the first excited state (10^5 times the experimental).

B. ^{25}Mg and ^{25}Al Nuclei (Refs. 45 to 62)

Figure 13 compares the theoretical results with the experimental data concerning the spectra of

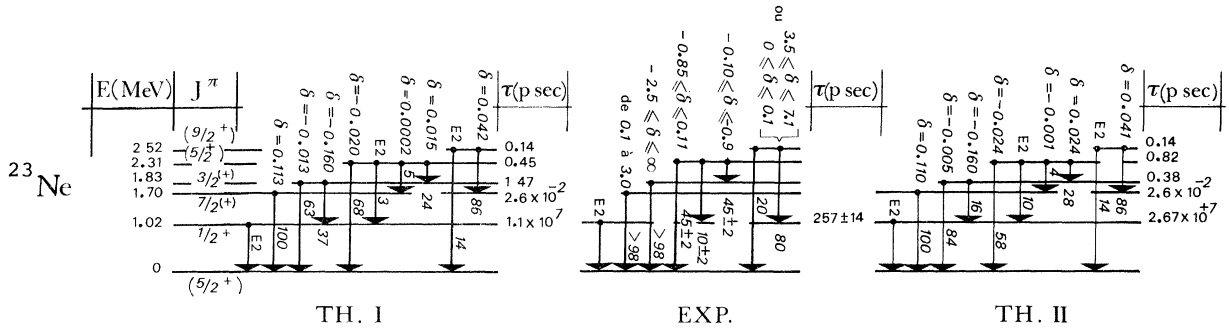

FIG. 12. Electromagnetic properties of the first P^+ states of ^{23}Ne. The experimental lifetime is from Ref. 44, the branching and mixing ratios are from Refs. 38, 41. The choice of the more probable J^π assignment for some levels is pointed out with parentheses.

the mirror pair ^{25}Mg-^{25}Al. The seven P^+ states of the energy sequence we have optimized are well reproduced in both versions of the model. Moreover, a $\frac{9}{2}^+$ theoretical level appears at 4.6 and 4.7 MeV in TH.I and TH.II, respectively. It might be related with the levels at 4.70 and 4.51 MeV in ^{25}Al and ^{25}Mg, rather than with the $\frac{9}{2}^+$ state at 4.05 and 4.04 MeV, respectively.[47] However, no other experimentally known P^+ state is well given by the model. Particularly, the three levels at 2.57 MeV ($\frac{1}{2}^+$), 2.81 MeV ($\frac{3}{2}^+$), and 3.91 MeV ($\frac{5}{2}^+$) in ^{25}Mg (and their analogs in ^{25}Al), usually interpreted as the first members of a rotational band,[45,47] are placed too high by the model, which however gives the required spacings between them. If we attempt the inclusion of one, two, or all three levels in the energy sequence to be fitted, bad results are obtained for the lower part of the spectrum. This example is characteristic of the known trend of the Nilsson model[3] to be at variance with the relative positioning of the rotational bands.

The P^- states appear from 5 MeV on, in version TH.I; this is therefore quite above the first three experimental negative-parity states, which lie between 3 and 4.3 MeV.[53] Modifying the inertia and deformation in the second version allowed us to find the experimental $\frac{3}{2}^-$, $\frac{7}{2}^-$, $\frac{1}{2}^-$ sequence.

The spectrum of the H^+ states starts off at 2.2 MeV in TH.I and a little higher in TH.II. The first H^- state appears at 7 MeV in TH.I and 5 MeV

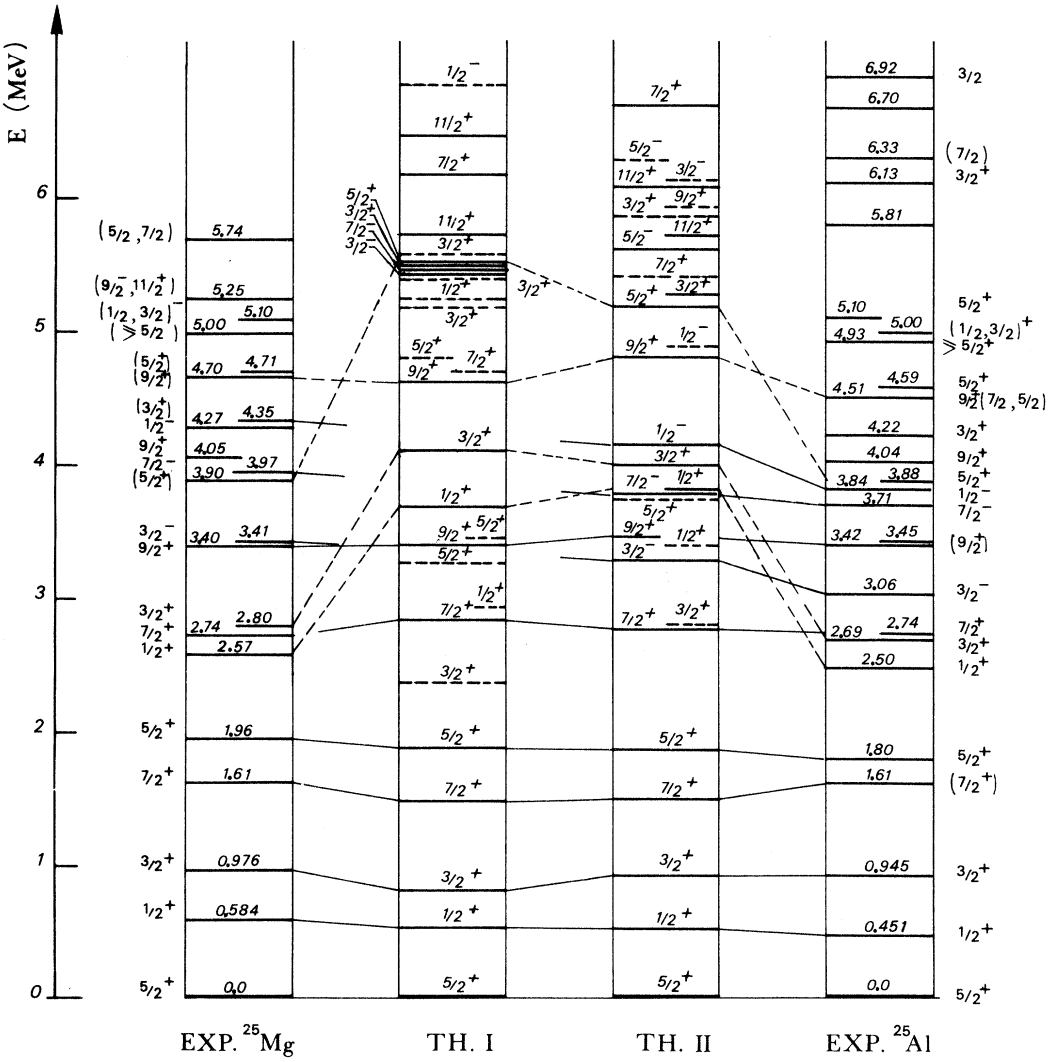

FIG. 13. Energy levels of ^{25}Mg and ^{25}Al. The experimental data below 5 MeV are taken from Ref. 45 for ^{25}Mg (except for the 4.05-MeV level, Ref. 46) and from Refs. 47 and 48 for ^{25}Al. Above 5 MeV, some results of Refs. 49–52 are quoted. The same notations as in Fig. 1 are used. The values of the fitting parameters and of the equilibrium deformations are given in Tables I and VII.

in TH.II. We thus encounter the same difficulties as for the other nuclei, since a hole-state interpretation has been proposed for the levels at 4.35 ($\frac{3}{2}^+$), 4.71 ($\frac{5}{2}^+$) according to Ref. 50, at 5.10 MeV ($\frac{1}{2}$, $\frac{3}{2}$)$^-$ according to Ref. 54, and at 4.22 MeV, $\frac{3}{2}^+$ and 4.59 MeV, $\frac{5}{2}^+$ according to Ref. 55.

Even if a modification of the parameters allowed a fit to these levels, several theoretical hole states—as the first $\frac{1}{2}^+$—would remain unrelated to experimental ones.

The same remarks as for ^{23}Ne may be made concerning the spectroscopic factors of ^{25}Mg (see Fig. 14). It still may be observed that the results concerning the $\frac{1}{2}^+$, $\frac{3}{2}^+$ states of the energetically shifted band are somewhat too large, especially in TH.I.

The static moments of the ground state are consistent in both versions of the model (see Table III). The magnetic moment of ^{25}Mg agrees with the experimental result, but the value found for the electric quadrupole moment is too small, owing to the relatively low deformation used for the whole nucleus in TH.I and for the orbit 5 in TH.II (see Tables I and VII).

Both versions of the model give quite similar results for the $E2$-$M1$ deexcitations of the first P^+ states (see Fig. 15). The calculated branching and mixing ratios of the levels introduced in the opti-

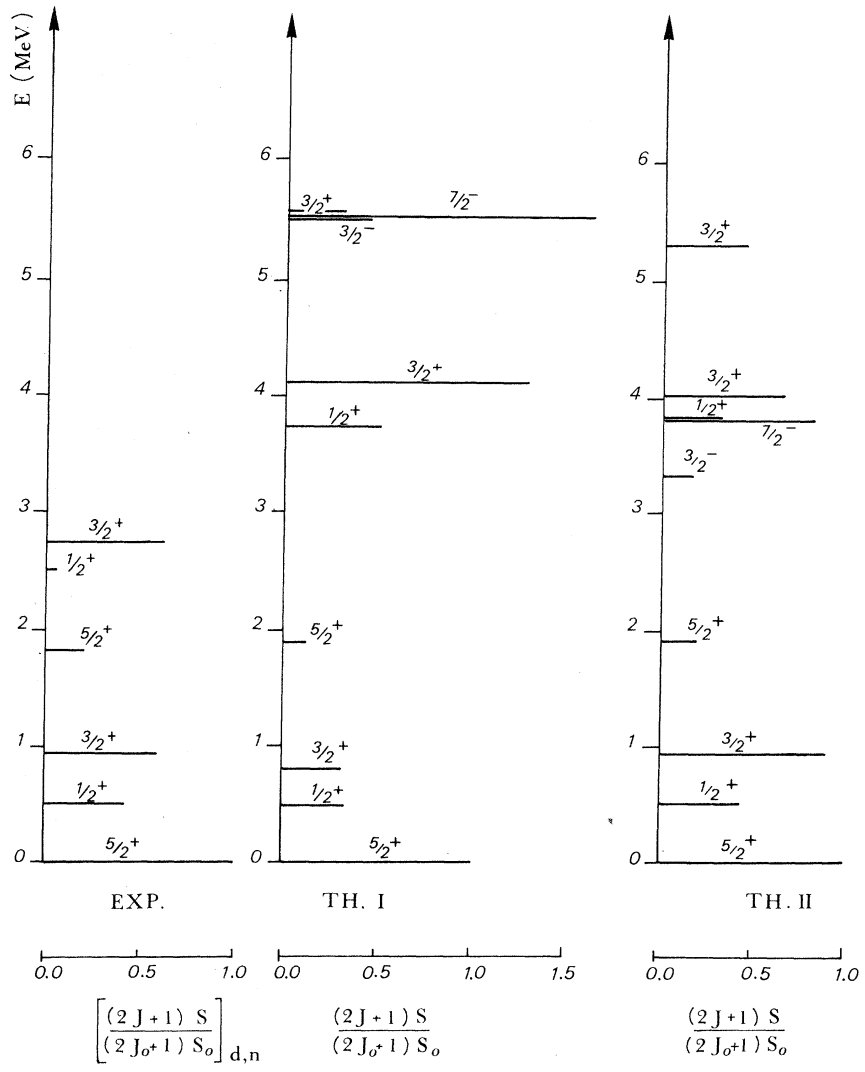

FIG. 14. Spectroscopic factors of ^{25}Mg and ^{25}Al. The experimental data correspond to the ^{24}Mg(d,n) reaction (Ref. 56). The theoretical value of $(2J+1)S$ for the ground state is 2.03 in both methods of calculation of the wave functions (TH.I and TH.II).

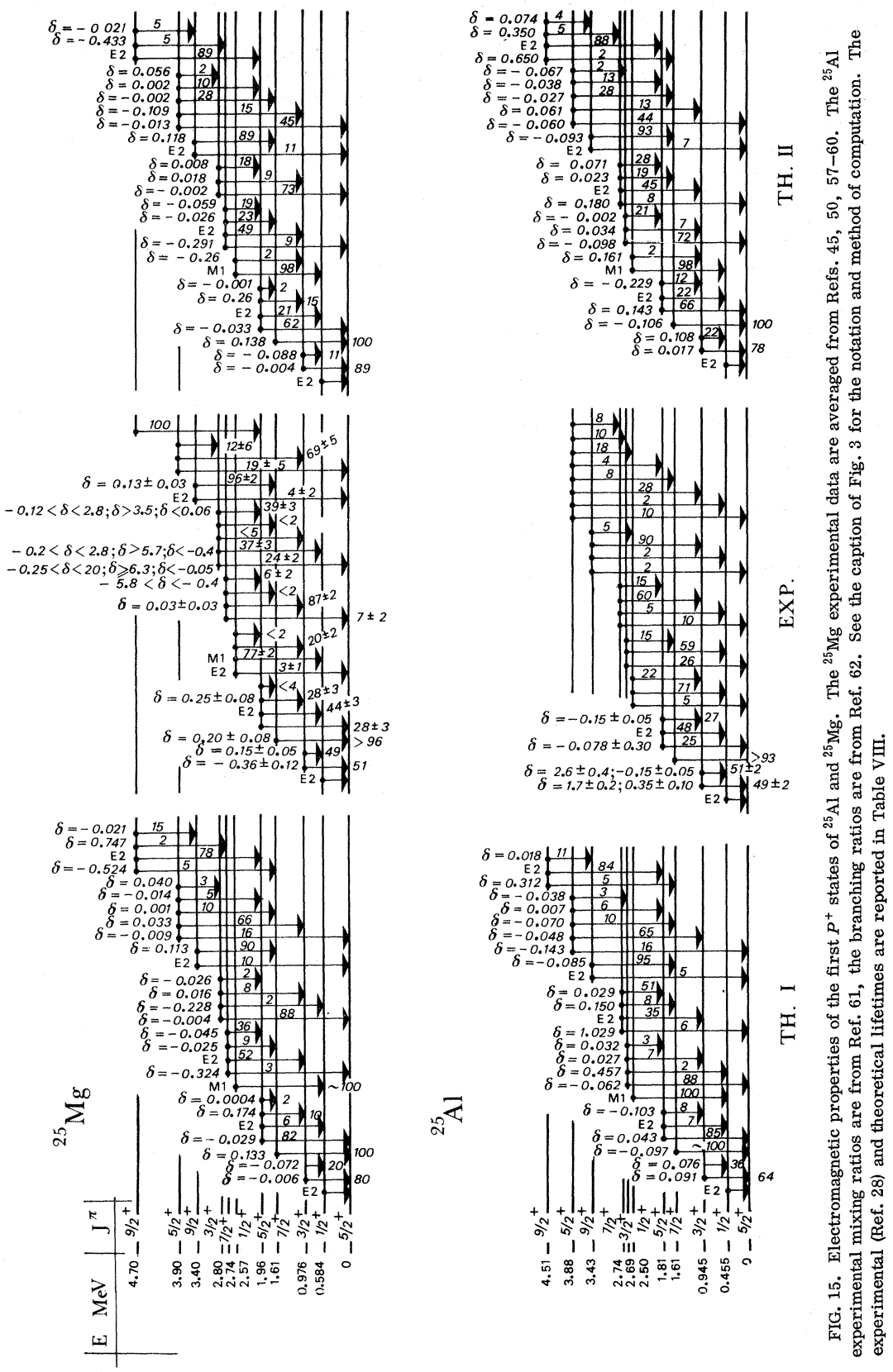

FIG. 15. Electromagnetic properties of the first P^+ states of ^{25}Al and ^{25}Mg. The ^{25}Mg experimental data are averaged from Refs. 45, 50, 57–60. The ^{25}Al experimental mixing ratios are from Ref. 61, the branching ratios are from Ref. 62. See the caption of Fig. 3 for the notation and method of computation. The experimental (Ref. 28) and theoretical lifetimes are reported in Table VIII.

TABLE VII. Equilibrium deformations $\eta(\epsilon)$ used in the second method of calculation (TH. II) for the ^{25}Mg-^{25}Al mirror pair [the value of $\eta(\epsilon)$ for the orbit 14 is not the equilibrium deformation, but is readjusted to fit experiment]. The fitting parameters are $\mu_{II}=0.19$ $\kappa_{II}=0.113$, $\hbar^2/2\mathcal{I}_{II}=217$ keV for all the orbits, except for the orbit 14 ($\hbar^2/2\mathcal{I}_{II}=100$ keV).

Core	With hole				Without hole				
Configuration of the core	$(13467)^4(25)^2$	$(12367)^4(45)^2$	$(12347)^4(56)^2$	$(12346)^4(57)^2$	$(123467)^4$				
Band based on the Nilsson orbit:	2	4	6	7	5	9	11	8	14
$\eta(\epsilon)$	2.2	2.1	1.1	1.8	2.4	3.1	2.6	2.5	2.2

mization sequence are in a semiqualitative agreement with experiment. The theoretical lifetimes are satisfactory but, as in ^{23}Ne, the value of the first excited state of ^{25}Mg is too large (about one hundred times) (see Table VIII). The second $\frac{9}{2}^+$ theoretical state does not decay according to the 4.05-MeV level in ^{25}Mg (4.04 MeV in ^{25}Al), but rather in a qualitative agreement with the deexcitation of the 4.70-MeV level in ^{25}Mg; this confirms the point of view mentioned above. The electromagnetic properties of the three levels building the energetically shifted band are less satisfactory than those of the remaining levels.

C. ^{27}Al and ^{27}Si Nuclei (Refs. 63 to 77)

Figure 16 shows a comparison between the experimental and theoretical spectra of the mirror pair ^{27}Al-^{27}Si. Notwithstanding the good knowledge of a number of P^+ states, we could only fit the first five. The agreement is quite good between TH.I, TH.II, and experiment for the optimized levels; it remains reasonable for the sixth experimental level at 2.98 MeV in ^{27}Al (and for its analog in ^{27}Si), and becomes less good for the $\frac{1}{2}^+$ experimental level at 3.68 MeV in ^{27}Al (and for the related level in ^{27}Si).

On the contrary, the remaining levels, especially the first experimental $\frac{9}{2}^+$, are very ill-reproduced in both versions of the model. All attempts carried out to fit a wider number of levels failed on account of increasing discrepancies in the lower part of the spectrum.

The calculation of the levels arising from the other configurations gave:

(i) The P^- states. The P^- states are above 7 MeV in TH.I, which is not too far from the 6.16- and 6.48-MeV levels in ^{27}Al, now interpreted as negative-parity states.[63] No attempt was made to get a better fit when using TH.II.

(ii) The H^+ states. Their spectrum begins at 2 MeV in TH.I, without any related experimental level at this energy. The version TH.II yields negative equilibrium deformation for these states (see Table IX), so they have not been studied in the frame of this version.

(iii) The H^- states. The H^- states appear at about 6 MeV in TH.I and 4 MeV in TH.II when taking into account in the latter version the positive deformation $\eta=0.1$ that brings the value of χ^2 to a minimum (see Table IX). The existence of the experimental states at 4.05 MeV in ^{27}Al and 4.13 MeV in ^{27}Si, interpreted now as negative-parity hole states,[67,70,71] is thus adequately justified without any modification of the parameters.

The calculated spectroscopic factors are compared in Fig. 17 to their experimental values for the ^{26}Mg(d,n) reaction up to 4 MeV. The agreement is qualitatively satisfactory in spite of discrepancies for the second and the first $\frac{3}{2}^+$ levels in TH.I and TH.II, respectively. Above 4 MeV, the model yields a strong spectroscopic factor for the $\frac{7}{2}^-$ level, which agrees with the measurements of Ref. 72 for the ^{26}Mg (^{3}He, d) reaction.

TABLE VIII. Lifetimes (in psec) of ^{25}Mg and ^{25}Al.

Nucleus	E (MeV)	$\tau_{TH.I}$	τ_{EXP}	$\tau_{TH.II}$
^{25}Mg	4.70	0.11		6.8×10^{-2}
	3.90	2.0×10^{-3}	<0.02	2.2×10^{-3}
	3.40	1.3×10^{-2}		1.3×10^{-2}
	2.80	7.9×10^{-3}	$(2.7\pm0.6)\times10^{-2}$	1.3×10^{-2}
	2.74	0.74	0.29 ± 0.02	0.34
	2.57	8.4×10^{-3}	$(5.9\pm2.6)\times10^{-2}$	6.9×10^{-3}
	1.96	0.43	$(6\pm1.8)\times10^{-1}$	0.68
	1.61	2.8×10^{-2}	$(2.5\pm0.6)\times10^{-2}$	2.8×10^{-2}
	0.976	3.9	16 ± 4	1.6
	0.584	1.5×10^{6}	$(5.0\pm0.6)\times10^{3}$	1.7×10^{6}
^{25}Al	4.51	0.10		6.3×10^{-2}
	3.88	1.4×10^{-3}		1.6×10^{-3}
	3.43	9.8×10^{-3}		9.7×10^{-3}
	2.74	0.43	0.45 ± 0.10	0.20
	2.69	6.2×10^{-3}		1.08×10^{-2}
	2.50	5.6×10^{-3}		4.6×10^{-3}
	1.81	0.39	0.55 ± 0.10	0.62
	1.61	2.2×10^{-2}	0.028 ± 0.06	2.1×10^{-2}
	0.945	2.41	>6	1.1
	0.455	3.4×10^{4}	2.29×10^{3}	2.2×10^{4}

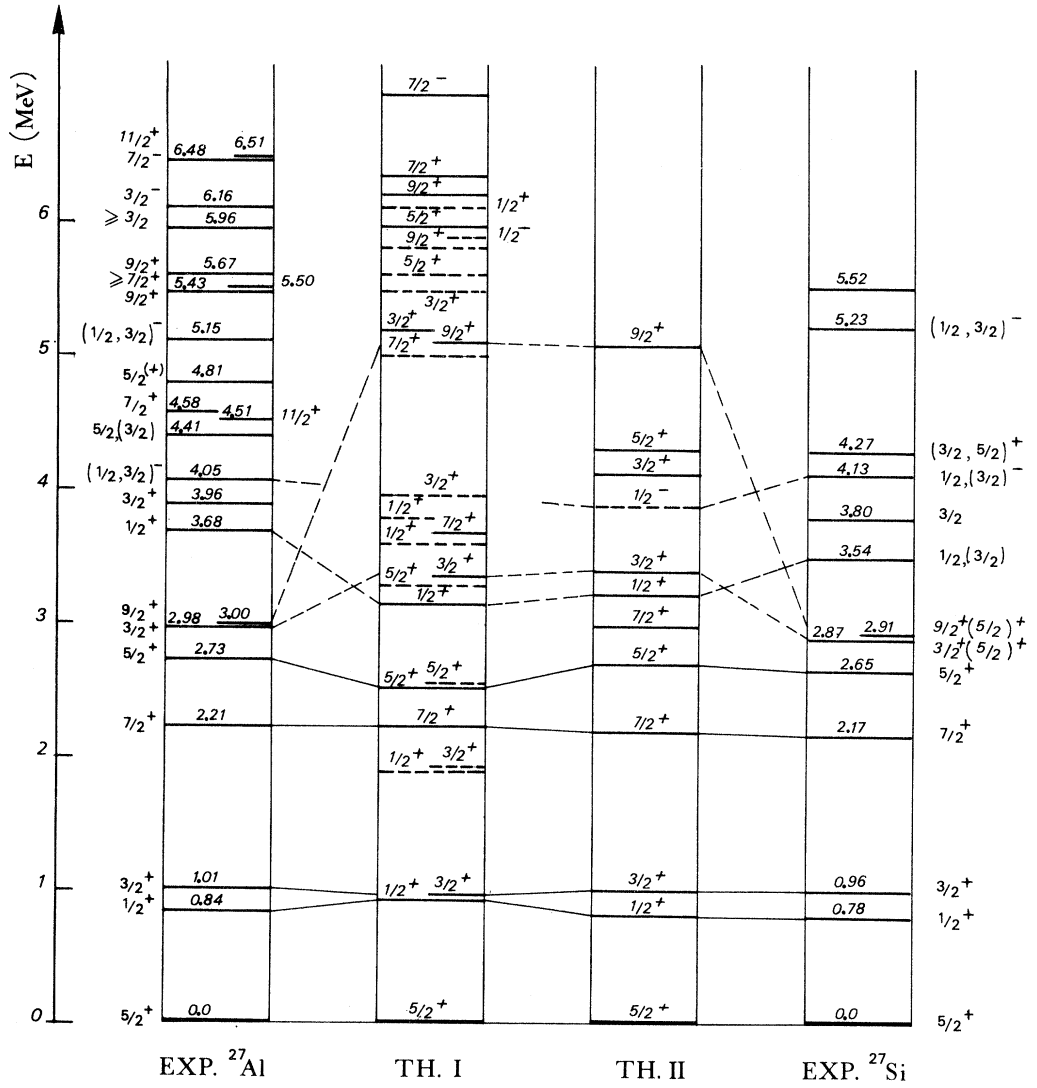

FIG. 16. Energy levels of ^{27}Al and ^{27}Si. The experimental data are from Refs. 63–65 for ^{27}Al and from Refs. 66–69 for ^{27}Si. The same notations as in Fig. 1 are used. The fitting parameters and the equilibrium deformations are given in Tables I and VIII.

The magnetic dipole moments of the fundamental are identical in both versions and agree well with the experimentally known value for ^{27}Al (see Table III). The electric quadrupole momentum as calculated for ^{27}Al is less than one half of its experimental value in TH.I and still lower in TH.II (less than one third); this is the poorest agreement we have obtained within both the $\xi = 11$ and $\xi = 13$

TABLE IX. Equilibrium deformations $\eta(\epsilon)$ used in the second method of calculation (TH. II) for the ^{27}Al-^{27}Si mirror pair (for the orbits 2 and 4, two values are found; that corresponding to the less sharp minimum of the static energy is indicated with parentheses). The fitting parameters are $\mu_{II} = 0.36$, $\kappa_{II} = 0.085$, and $\hbar^2/2\mathcal{J}_{II} = 317$ keV for all the orbits.

Core	With hole				Without hole			
Configuration of the core	$(134567)^4(2)^2$	$(123567)^4(4)^2$	$(12345)^4(6)^2$	$(123456)^4(7)^2$	$(123467)^4(5)^2$			
Band based on the Nilsson orbit:	2	4	6	7	5	9	11	8
$\eta(\epsilon)$	1.1(−4.6)	(0.1) −6.4	−4.4	−4.7	1.6	2.9	1.9	1.8

series of nuclei.

The calculated $E2$-$M1$ deexcitations of the first P^+ states are compared with experiment on Fig. 18. The two versions of the models predict similar results. The lifetimes are satisfactory on the whole, except as concerns the first excited state, to which—as in the other $\xi = 13$ nuclei we have studied—is attributed a far too large value of τ (by a factor of 10^2 for ^{27}Al and 10^4 for ^{27}Si). The branching ratios are good for the first half of the reported levels. But they are in disagreement with experiment for (i) the first excited $\frac{5}{2}^+$ state, which is yet well located in energy, and (ii) the second $\frac{1}{2}^+$ and—mainly— $\frac{9}{2}^+$ states which are both shifted in the energy spectrum. The mixing ratios are generally in poor agreement with experiment;

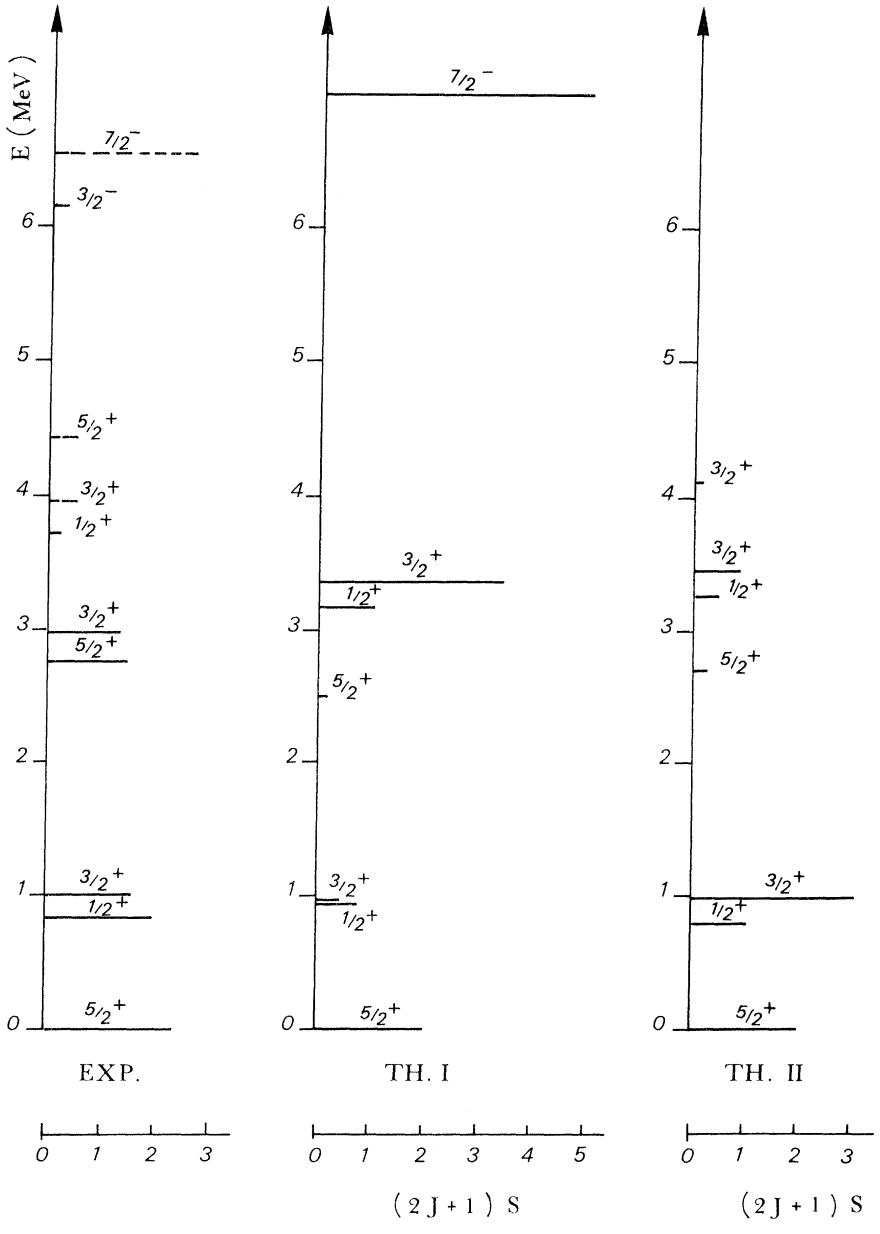

FIG. 17. Spectroscopic factors of ^{27}Al and ^{27}Si. On the left part of the figure (EXP) and below 3.7 MeV, the solid lines refer to $(2J+1)S$ for the ^{26}Mg(d,n) reaction (Ref. 49). Above, the dashed lines refer to $(2J+1)C^2S$ for the ^{26}Mg$(^3$He$,d)$ reaction (Ref. 72).

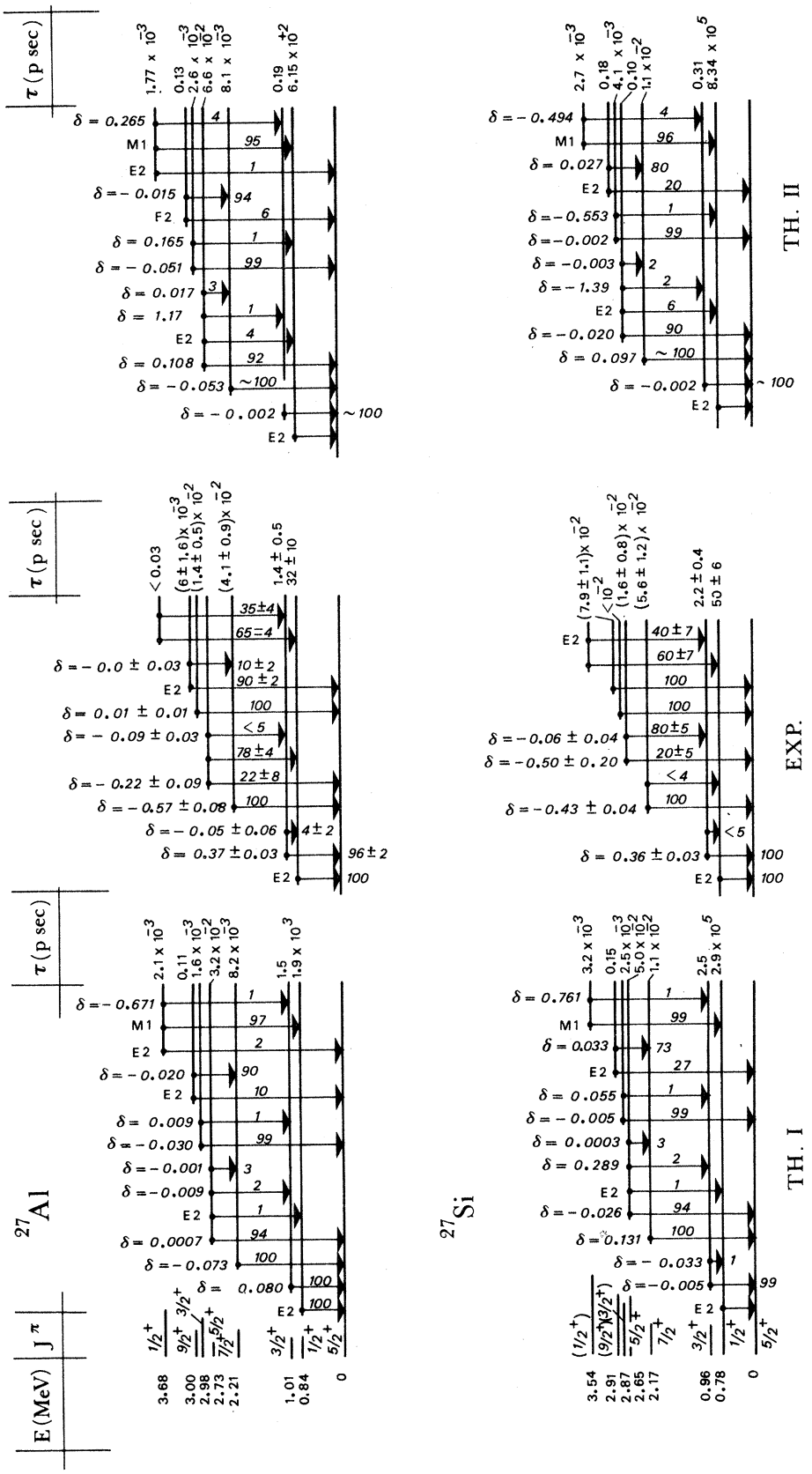

FIG. 18. Electromagnetic properties of the first P^+ states of ^{27}Al and ^{27}Si. The experimental data are from Refs. 49, 63, 73, 77 for ^{27}Al and Refs. 66 (branching and mixing ratios) and 68 (lifetimes) for ^{27}Si.

TABLE X. Comparison of the parameters obtained by the two methods of calculation (TH. I and TH. II) for the P^+ states (the subscripts I and II correspond to TH.I and TH.II, respectively). As concerns the nuclei with an odd number of nucleons $\xi = 11$, the deformation δ_{II} is calculated from the average of the $\eta(\epsilon)$ parameter values given for the orbits 7, 5, 9, 11, 8 in Tables II–V; for $\xi = 13$ the average of the $\eta(\epsilon)$ values given for the orbits 5, 9, 11, 8 in Tables VI–VIII is used. $\hbar^2/2\mathcal{J}$ is in keV. See these tables for the other configurations.

	δ_I	δ_{II}	μ_I	μ_{II}	κ_I	κ_{II}	$\hbar^2/2\mathcal{J}_I$	$\hbar^2/2\mathcal{J}_{II}$
^{19}O	0.159	0.170	0.0046	0.013	0.078	0.081	294	310
^{21}Ne-^{21}Na	0.243	0.300	0.0675	0.050	0.089	0.115	250	253
^{23}Na-^{23}Mg	0.325	0.295	0.106	0.175	0.079	0.10	205	235
^{23}Ne	0.246	0.273	0.082	0.095	0.114	0.139	234	235
^{25}Mg-^{25}Al	0.239	0.276	0.173	0.19	0.088	0.113	215	217
^{27}Al-^{27}Si	0.164	0.168	0.254	0.36	0.074	0.085	320	317

contrasting with the preceding results obtained for the other nuclei, some of their signs are not even correctly reproduced.

V. DISCUSSION

A. Summary of Results

The theoretical predictions of the phenomenological models of Bohr-Mottelson and Nilsson are found here to be, in general, in rather good agreement with the experimental data concerning the five $\xi = 11$ nuclei: ^{19}O, ^{21}Ne, ^{21}Na, ^{23}Na, ^{23}Mg, and the five $\xi = 13$ nuclei: ^{23}Ne, ^{25}Mg, ^{25}Al, ^{27}Al, ^{27}Si. This agreement is particularly good for the energies of the first P^+ states, which is consistent with the fact that the values of the parameters have been fitted to reproduce these P^+ energies (see Table X and Fig. 19). Furthermore, the theoretical spectra yield identification for other nonoptimized levels. However, some theoretical P^+

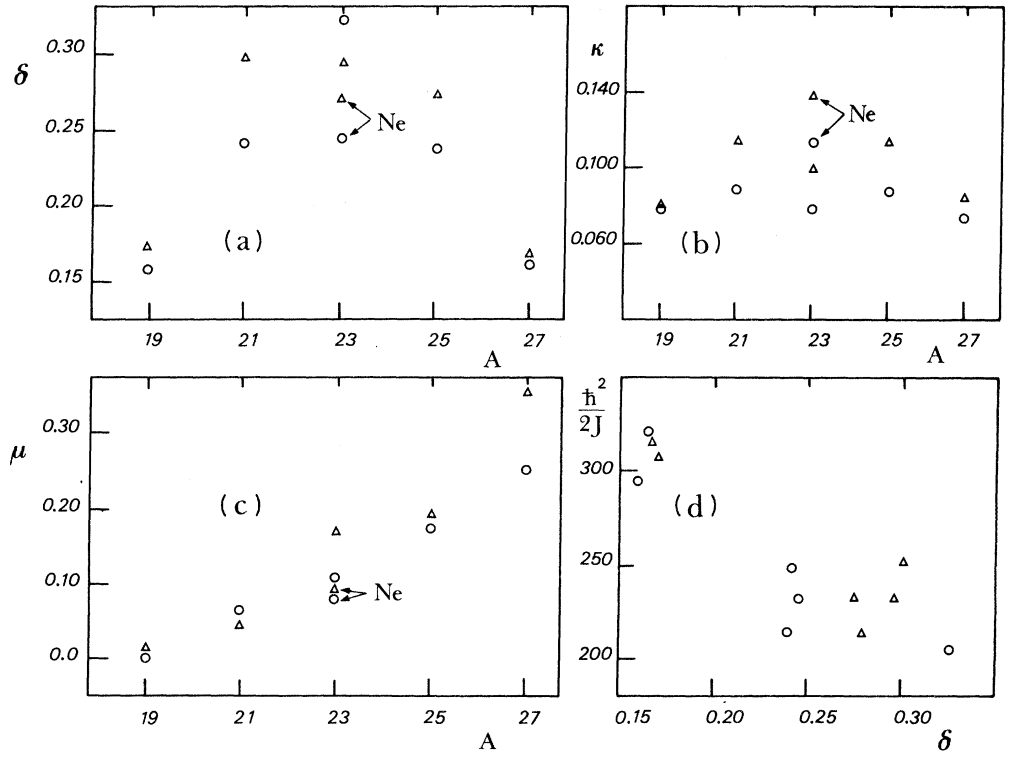

FIG. 19. Parameters of the model for the P^+ states (○ TH.I, △ TH.II) (the numerical values are taken from Table VI). The deformation δ, the spin-orbit coupling strength κ, and the l^2-term parameter μ are plotted versus the mass number A respectively in (a), (b), (c). Figure 19(d) shows the inverse of the moment of inertia ($\hbar^2/2\mathcal{J}$ in keV) plotted versus the deformation.

levels (e.g., first $\frac{7}{2}^+$ in ^{19}O, second $\frac{3}{2}^+$ in ^{21}Na) have theoretical energies very different from their experimental values. Finally, the experimental values of the spectroscopic factors are well reproduced by both TH.I and TH.II formulations of the model for the $A=21$ and 27 nuclei and more qualitatively for the $A=19$ nucleus.

The calculated electromagnetic properties (static moments of the ground state, lifetimes, branching and mixing ratios of the P^+ states) are consistent in both descriptions. The few deviations are essentially due to the various values of the deformation used for the different Nilsson orbits in the TH.II model (see Tables II, V, VI, VII, and IX). The agreement with experiment is, on the whole, satisfactory. However, discrepancies occur for some levels which are already shifted in energy (e.g., $\frac{3}{2}^+$ at 4.47 MeV in ^{21}Na spectrum) in spite of our introducing the experimental energies in the transition formula [Eq. (13)]. Deviations from experiment occur too for the $\frac{1}{2}^+$, $\frac{3}{2}^+$ levels at 2.39- and 2.98-MeV energies, respectively, in ^{23}Na (and the corresponding states in ^{23}Mg) which have good theoretical energies. Thus, calculating the energies correctly seems to be a necessary but insufficient condition to give wave functions leading to satisfactory γ transition results. Discrepancies occur too for the lifetimes of the first excited levels of $\xi=13$ nuclei.

We calculated the other excited states, members of the P^-, H^+ configurations, and we found it difficult to place them correctly one with respect to the other. The two methods TH.I and TH.II lead to rather different results concerning the relative positions of the configuration heads; the agreement with experiment seems fortuitous. Roughly speaking, the theoretical energies of the H^+ states are too low. This inconvenience could possibly be removed by allowing a certain amount of mixing between the P^+ and H^+ states. This mixing is probably not very important because the corresponding cores differ by two occupied orbits, but is not rigorously negligible. Such a mixing with P^+ and H^+ does not exist for H^- states because of parity conservation; this could explain the better interpretation (in TH.II) for the H^- than for the H^+ states, but cannot account for the differences between TH.I and TH.II concerning these states. Finally, the theoretical energies of the P^- states are found to be generally too important. However, (i) the second calculation (TH.II) reproduces the experiment for $A=21$, providing that the deformation is a fitting parameter different from its equilibrium value but close to the average deformation of the other orbits; (ii) the first calculation (TH.I) reproduces the experiment for $A=23$ without any additional parameter, provided that one at least of the negative-parity 5.97- and 6.91-MeV states in ^{23}Na be a particle state. The unsatisfactory positioning of the P^- states may be owed to the fact that we neglected the Coriolis mixing with $1p$ states in both versions and in the $2p$-$1f$ shell in TH.II, notwithstanding the important deformation.

B. Concluding Remarks

The present investigation of the 10 nuclei with $\xi=11$ or 13 allows us to make the following observations. First of all, it should be remembered that in TH.II the deformation parameter is not adjusted to reproduce energy levels as in TH.I, but is determined from a calculation of the minimum static energy and thus corresponds to an equilibrium shape. Now, it is important to notice that both versions of the model give consistent results for the energies and wave functions of the P^+ states. So, the additional constraint imposed on the deformation parameter in TH.II does not deteriorate the agreement between the model predictions in TH.I and the experiment (see an illustrative example in Table XI). This result probably emphasizes the physical meaning of the constraint leading to the determination of the effective deformation which therefore corresponds to an equilibrium of the nuclear shape. Thus, one may conclude that the Nilsson model allows a correct description of the variations of the total nuclear static energy versus the deformation. Unfortunately, it does not allow a correct comparison of the total static energies related to various core configurations. We noticed indeed the trend of the Nilsson model to be in disagreement with the relative positioning of the rotational bands belonging to different core configuration and even—as an exception—of a special rotational band in the P^+ configuration (see Sec. IV B on ^{25}Al-^{25}Mg). However, the Nilsson model is strictly a particle-independent model which does not take into account any specific pairing energy and any cluster formation. Though the orbit-filling procedure we used is an aspect of pairing the nucleons in orbits, the

TABLE XI. Values of the minimum obtained for the least-squares error between observed and model-predicted energies of the P^+ states of the nuclei with an odd number of nucleons $\xi=11$ and $\xi=13$. The optimized sequences of levels are indicated on the figures showing the energy spectra. χ_I^2 and χ_{II}^2 (in MeV^2) refer to the first and second method of calculation.

	^{19}O	^{21}Ne-^{21}Na	^{23}Na-^{23}Mg	^{23}Ne	^{25}Mg-^{25}Al	^{27}Si-^{27}Al
χ_I^2	1.4	2.4	0.47	0.023	0.043	5×10^{-2}
χ_{II}^2	1.3	2.5	0.41	0.015	0.013	2×10^{-4}

pairing energies do not have to be the same for the different core configurations. Neglecting such variations of the pairing energy is probably unjustified.

It is useful to emphasize that all the theoretical results discussed above have been obtained with a very small number of parameters: the spin-orbit coupling-strength parameter κ and the l^2-term parameter μ in the Nilsson Hamiltonian. To these parameters we add two other ones in the first formulation of the model: the deformation δ and the inverse momentum of inertia ($\hbar^2/2\mathcal{J}$), taking the same values for all states in a nucleus. In the second formulation of the model, the deformation $\eta(\epsilon)$ is no more a fitting parameter but the moment of inertia is sometimes allowed to have a particular value for each configuration. The values of the parameters obtained in both formulations are close together in the same neighborhood for all 10 nuclei and quite consistent with previous studies in the same mass region (see Table X and Fig. 19); i.e., (i) the deformation is positive (cigar-shaped nuclei), (ii) μ increases with the mass number from almost zero ($A=19$) to about 0.30 ($A=27$), (iii) κ is fluctuating in the small range 0.08–0.14, and (iv) $\hbar^2/2\mathcal{J}$ goes smaller with the deformation and remains between 200 and 350 keV.

The properties of radiative transitions of the 10 nuclei are well reproduced, on the whole, by the model. This fact indicates that the Nilsson wave functions for the intrinsic states reasonably describe the actual states. Besides, their similarity with the Hartree-Fock states has been emphasized very often. This property comes from the validity of the energy decomposition into a rotational and an intrinsic part as realized by Bohr and Mottelson, in the case of the Nilsson intrinsic potential applied to the description of the lower $2s$-$1d$ shell nuclei.

The present investigation confirms that the even-odd nuclei with an odd number of nucleons, $\xi=11$ or 13 (except ^{19}O, which is not yet experimentally well known and may be nonaxial), show prolate deformation corresponding to an equilibrium rigid nuclear shape and can very satisfactorily be accounted for by the Bohr-Mottelson and Nilsson models.

Nevertheless, it would be of interest to find a method allowing, without any additional fitting parameter, the inclusion of the pairing effect and the correct placement of the various configurations with respect to one another. Thus, it would be consistent to investigate the electromagnetic decays of the H^+ states and of the P^- states, eventually including the Coriolis-coupling term in the $2p$-$1f$ shell.

C. Microscopic Considerations

The present study may guide calculations in less phenomenological models and even assist in understanding the success or failures of these calculations. In the so-called microscopic studies, and particularly in the Hartree-Fock method (HF), the choice of a conveniently truncated basis is a prominent problem. In the study of a given nucleus by the HF method, it seems advisable to choose a basis constituted by the eigenstates of a deformed harmonic oscillator with a deformation resulting from a phenomenological calculation like ours. Further, the $\vec{l}\cdot\vec{s}$ coupling term which is sometimes included in the HF potential might be chosen in the same manner. Finally, in an iterative HF-type calculation, one may take for the occupied states as a starting point the Nilsson states corresponding to one of the allowed intrinsic configurations. Then, each configuration $C^{(i)}$ leads to an HF wave function $\psi^{(i)}$ from which eigenstates of angular momentum $\psi^{(i)}_{JM}$ are projected. These $\psi^{(i)}_{JM}$ favorably replace the states of a Bohr-Mottelson rotational band. Instead of mixing the bands by the Coriolis term, one advantageously diagonalizes the Hamiltonian on the basis constituted by the projected states $\psi^{(i)}_{JM}$ which correspond to the various intrinsic wave functions $\psi^{(i)}$.

It follows that the success of such HF calculations will be greater, without introducing too many configurations, if the assumed intrinsic structures have a better physical foundation. The phenomenological calculations allow us to know precisely whether the nucleus shows an important stable deformation and consequently actual intrinsic configurations. For the nuclei investigated here, it thus seems that HF calculation might be successful assuming a suitable choice of the potential. However, while many of the calculations have been performed on the neighboring even-even nuclei, only a few attempts have been made for these even-odd nuclei (see Ref. 78, for example), perhaps because finding a convenient potential is not easy in this case.

---

*Now at Laboratoire de Physique Théorique et Hautes Energies, Université de Paris XI, Centre d'Orsay, France.

[1]A. Bohr, K. Dan. Vidensk. Selsk. Mat.-Fys. Medd. 26, No. 14 (1952); A. Bohr and B. R. Mottelson, *ibid.* 27, No. 16 (1953).

[2]S. G. Nilsson, K. Dan. Vidensk. Selsk. Mat.-Fys. Medd. 29, No. 16 (1955).
[3]K. H. Bhatt, Nucl. Phys. 39, 375 (1962).
[4]B. E. Chi and J. P. Davidson, Phys. Rev. 131, 366 (1963).
[5]M. A. Melkanoff, T. Sawada, and J. Raynal, Methods in Computational Physics (Academic, New York, 1966), Vol. 6, p. 50.
[6]W. Scholz and F. B. Malik, Phys. Rev. 147, 836 (1966); Phys. Rev. 150, 919 (1966); Phys. Rev. 153, 1071 (1967).
[7]P. Desgrolard, thèse de 3ème cycle, Univ. de Lyon, Lycen-7177 (1971).
[8]J. P. Boisson and R. Piepenbring, Nucl. Phys. A168, 385 (1971).
[9]J. A. Nelder and R. Mead, Comput. J. 7, 308 (1965).
[10]M. Lambert, G. Dumazet, H. Beaumevieille, A. Tellez, C. Meynadier, and P. Midy, Nucl. Phys. A112, 161 (1968).
[11]P. Midy, thèse de 3ème cycle, Univ. de Lyon, Lycen-7071 (1970).
[12]H. J. Rose and D. M. Brink, Rev. Mod. Phys. 39, 306 (1967).
[13]B. C. Carlson and I. Talmi, Phys. Rev. 96, 436 (1954).
[14]F. Hibou, P. Fintz, B. Rastegar, and A. Gallmann, Nucl. Phys. A171, 603 (1971).
[15]M. Fasla and H. Beaumevieille, Nuovo Cimento 9A, 547 (1972).
[16]R. E. McDonald, D. B. Fossan, L. F. Chase, Jr., and J. A. Becker, Phys. Rev. 140, B1198 (1965).
[17]C. Broude, U. Karfunkel, and Y. Wolfson, Nucl. Phys. A161, 241 (1971).
[18]R. E. McDonald, J. A. Becker, and A. D. W. Jones, Phys. Rev. C 4, 377 (1971).
[19]P. Fintz, F. Hibou, B. Rastegar, and A. Gallmann, Nucl. Phys. A132, 265 (1970).
[20]J. F Allard, S. Bendjaballah, P. Desgrolard, and T. F. Hammann, Nuovo Cimento 9A, 561 (1972).
[21]A. J. Howard, J. G. Pronko, and C. A. Whitten, Jr., Nucl. Phys. A152, 317 (1970).
[22]C. Rolfs, E. Kuhlmann, F. Riess, and R. Kramer, Nucl. Phys. A167, 449 (1971).
[23]M. Lambert, P. Midy, D. Drain, M. Amiel, H. Beaumevieille, A. Dauchy, and C. Meynadier, J. Phys. (Paris) 33, 155 (1972).
[24]M. B. Burbank, G. G. Frank, N. E. Davison, G. C. Neilson, S. M. Wong, and W. J. McDonald, Nucl. Phys. A119, 184 (1968).
[25]B. J. Cole, Phys. Lett. 33B, 321 (1970).
[26]J. G. Pronko, R. A. Lindgren, and D. A. Bromley, Nucl. Phys. A140, 465 (1965).
[27]R. Bloch, T. Knellvolf, and R. E. Pixley, Nucl. Phys. A123, 129 (1969).
[28]A. Bamberger, K. P. Lieb, B. Povh, and D. Schwalm, Nucl. Phys. A111, 12 (1968).
[29]K. Bharuth-Ram, K. P. Jackson, K. W. Jones, and E. K. Warburton, Nucl. Phys. A137, 262 (1969).
[30]R. A. Lindgren, R. G. Hirko, J. G. Pronko, A. T. Howard, M. W. Sachs, and D. A. Bromley, Nucl. Phys. A180, 1 (1972).
[31]L. C. Haun, N. R. Roberson, and D. R. Tilley, Nucl. Phys. A140, 333 (1970).
[32]R. Engmann, F. Brandolini, and I. Mauritzon, Nucl. Phys. A171, 418 (1971).
[33]J. Dubois, Nucl. Phys. A104, 657 (1967).
[34]M. Arditi, L. Bimbot, H. Doubre, N. Frascaria, J. P. Garron, M. Riou, and D. Roger, Nucl. Phys. A165, 129 (1971).
[35]A. R. Poletti, A. D. W. Jones, J. A. Becker, R. E. McDonald, and R. W. Nightingale, Phys. Rev. 184, 1130 (1969).
[36]J. Dubois, Nucl. Phys. A116, 489 (1968).
[37]H. J. Maier, J. G. Pronko, and C. Rolfs, Nucl. Phys. A146, 99 (1970).
[38]H. Nann, R. Bass, K. O. Groneveld, and F. Saleh-Bass, Z. Phys. 218, 190 (1969).
[39]H. F. Lutz, J. J. Wesolowsky, L. F. Hansen, and S. F. Eccles, Nucl. Phys. A95, 591 (1967).
[40]G. A. Keyworth, P. Wilhjelm, G. C. Kyker, H. W. Newson, and E. G. Pilpuch, Phys. Rev. 176, 1302 (1968).
[41]A. T. Howard, J. P. Allen, D. A. Bromley, J. W. Olness, and E. K. Warburton, Phys. Rev. 154, 1067 (1967).
[42]E. Selin, Phys. Scr. 2, 169 (1970).
[43]M. Chambon, D. Drain, M. Yaker, G. Dumazet, G. Salmer, M. Beaumevieille, and M. Lambert, Nucl. Phys. A136, 311 (1969).
[44]D. B. Fossan, R. E. McDonald, and L. F. Chase, Jr., Phys. Rev. 141, 1018 (1966).
[45]J. F. Sharpey-Schafer, R. W. Ollerhead, A. J. Ferguson, and A. E. Litherland, Can. J. Phys. 46, 2039(1968).
[46]D. C. Kean and R. W. Ollerhead, Can. J. Phys. 49, 2793 (1971).
[47]H. Röpke, N. Anyar-Weiss, and A. E. Litherland, Can. J. Phys. 46, 2789 (1968).
[48]H. Röpke, N. Anyar-Weiss, and A. E. Litherland, Phys. Lett. 27B, 368 (1968).
[49]P. M. Endt and C. Van der Leun, Nucl. Phys. A91, 472 (1967).
[50]D. B. Sowerby, D. M. Sheppard, and W. C. Olsen, Nucl. Phys. A121, 181 (1968).
[51]J. R. Duray, H. J. Hansman, G. K. Marshall, J. W. Sinclair, and W. S. Steiner, Nucl. Phys. A136, 153 (1969).
[52]H. Röpke, H. J. Brundiers, and G. Hammel, Nucl. Phys. A153, 211 (1970).
[53]A. E. Litherland, H. McManus, E. B. Paul, D. A. Bromley, and H. E. Gove, Can. J. Phys. 36, 378 (1958).
[54]D. Dehnbard and J. L. Yntema, Phys. Rev. 160, 964(1967).
[55]B. R. Mottelson and S. G. Nilsson, K. Dan. Vidensk. Selsk. Mat.-Fys. Skr. 1, No. 8 (1959).
[56]H. Fuchs, K. Grabisch, P. Kraaz, and G. Roschert, Nucl. Phys. A110, 65 (1968).
[57]B. D. Sowerby and G. J. McCallum, Nucl. Phys. A112, 453 (1968).
[58]G. J. McCallum, Phys. Rev. 123, 568 (1961).
[59]G. J. McCallum and B. D. Sowerby, Phys. Lett. B25, 109 (1967).
[60]D. J. Donahue and R. L. Hershberger, Phys. Rev. C 4, 1693 (1971).
[61]N. Anyas-Weiss and A. E. Litherland, Can. J. Phys. 47, 2609 (1969).
[62]R. J. Van Reenen, Z. B. Dutoit, and W. L. Mouton, Z. Phys. 227, 326 (1969).
[63]P. J. M. Smulders, C. Broude, and J. F. Sharpey-Schafer, Can. J. Phys. 46, 2039 (1968).
[64]H. Röpke, V. Glattes, and G. Hammel, Nucl. Phys. A172, 506 (1971).

[65]M. J. A. De Voigt, J. Grottenhuis, J. B. Van Meurs, and C. Van der Leun, Nucl. Phys. A170, 467 (1971).
[66]M. B. Lewis, N. R. Roberson, and D. R. Tilley, Phys. Rev. 163, 1238 (1967).
[67]R. L. Kozub, Phys. Rev. 172, 1078 (1968).
[68]I. Mauritzson, R. Engmann, F. Brandolini, and V. Barci, Nucl. Phys. A174, 572 (1971).
[69]J. J. Weaver, D. A. Hutcheon, D. F. H. Start, R. W. Zürmühle, and M. A. Grace, Nucl. Phys. A172, 577 (1971).
[70]B. H. Wildenthal and E. Newman, Phys. Rev. 167, 1027 (1967).
[71]W. Parker-Alford, D. Cline, H. E. Gove, K. H. Parser, and S. Skorka, Nucl. Phys. A100, 333 (1967).
[72]H. W. Lutz, D. W. Heikkinen, W. Bartolini, and T. H. Curtis, Phys. Rev. C 2, 981 (1970).
[73]C. Van der Leun, D. M. Sheppard, and P. M. Endt, Nucl. Phys. A100, 316 (1967).
[74]D. M. Sheppard and C. Van der Leun, Nucl. Phys. A100, 333 (1967).
[75]H. Röpke and S. T. Lam, Can. J. Phys. 46, 1649 (1968).
[76]H. Röpke and N. Anyas-Weiss, Can J. Phys. 47, 1547 (1969).
[77]A. H. Lumpkin, K. A. Hardy, Y. K. Lee, and G. E. Owen, Phys. Rev. C 4, 1215 (1971).
[78]I. P. Johnstone and H. G. Benson, Nucl. Phys. A134, 68 (1969).